



Development and Validation of HPLC Assay Method for Etoricoxib in Bulk Drug and Tablet Formulation.

Gangane P.S*, S.M.Bagde,S.G.Mujbaile and K.D.Niranjane.

Department of Pharmaceutics, Dadasaheb Balpande College of Pharmacy, Nagpur-440034,(MS)India.

Received: 15 April 2014

Revised: 20 May 2014

Accepted: 30 May 2014

*Address for correspondence

P.S.Gangane,
Assistant Professor,
Dept. of Pharmaceutics,
Dadasaheb Balpande College of Pharmacy,
Besa, Nagpur-440034 (M.S.)India.
E.mail: p.gangane@rediffmail.com



This is an Open Access Journal / article distributed under the terms of the **Creative Commons Attribution License (CC BY-NC-ND 3.0)** which permits unrestricted use, distribution, and reproduction in any medium, provided the original work is properly cited. All rights reserved.

ABSTRACT

A simple, precise and specific high performance liquid chromatographic method was developed and validated for the determination of Etoricoxib in bulk and tablet dosage form. The method employed LC-10 ATVP Shimadzu Liquid Chromatograph HPLC with Hyper ODS 2 C18 size 4.5x250mm column as a stationary phase. The solvent system consists of Methanol (HPLC Grade) at flow rate 1 ml/min. The analysis of Etoricoxib was carried out at 233 nm. The calibration curve for Etoricoxib was linear from 20-55 µg/ml. The interday and intraday precision was found to be within limits. The proposed method has adequate sensitivity, reproducibility and specificity for the determination of Etoricoxib in bulk and its tablet dosage forms. LOD and LOQ for Etoricoxib were found to be 0.250 and 0.650. Accuracy (recoveries: 99.50-99.73 %) and reproducibility were found to be satisfactory.

Key words: Etoricoxib, HPLC Method, Methanol, Validation.

INTRODUCTION

Etoricoxib is a non steroidal anti inflammatory drug and highly COX-2 inhibitor[1-5]. Etoricoxib, 5-chloro-6'-methyl-3-[4-(methylsulfonyl) phenyl]-2, 3'-bipyridine, produces dose dependent inhibition of COX-2 without inhibition of COX-1. COX-2 inhibition provides anti-inflammatory and analgesic effects[6,7]. It is an off-white crystalline powder, relatively insoluble in water, and freely soluble in alkaline aqueous solution[3]. Etoricoxib is available in tablet dosage forms (60, 90, 120 mg) [4] and is not official in any pharmacopoeia. It is used for symptomatic management of

**Gangane et al.**

osteoarthritis [8-12],rheumatoid arthritis[13]and also indicated in primary dysmenorrhoea, postoperative dental pain, acute gouty arthritis, cancer treatment and prevention and migraine. It was found that some analytical methods such as Visible, UV, HPLC other methods were reported for Etoricoxib[14-16].The objective of the present study is to develop simple and accurate method for the determination of Etoricoxib by HPLC method in bulk drug and Tablet dosage form[17].

MATERIALS AND METHODS

Chemicals and Materials

All solvents were of HPLC grade. All other materials were purchased of analytical grade E-Merck, Qualigens, and Rankem etc. Distilled water and Whatman filter paper Grade-I were used throughout the experimental work. A Standard Etoricoxib compound was procured as a gift sample from Zim Lab.Ltd.Nagpur. The marketed formulations were purchased from the local market.

HPLC Instrumentation

LC-10 AT VP Shimadzu Liquid Chromatograph HPLC with Hyper ODS 2 C18 (size 4.6mmx250mm, particle size 5 μ m) column was used for the study. SPD-10 AVP Shimadzu UV-Visible is used as a detector and Shimadzu PU 2080 plus was the solvent delivery system. The system control and data processing were performed by ANALCROM software(Table1).

Mobile Phase

The mobile phase consists of Methanol HPLC Grade and the flow rate was 1 ml/min.

Preparation of standard drug solution

Stock solution of the drug (pure) is prepared by dissolving 25mg of Etoricoxib (Fig.1) in 25 ml of Methanol (HPLC Grade, MERCK) in 25ml volumetric flasks. Daily working standard solution of Etoricoxib were prepared between the ranges of 20-55 μ g/ml with mobile phase.

Calibration curves of Etoricoxib

Serial standard eight different concentration levels of Etoricoxib (20-55 μ g/ml) were prepared. For HPLC analysis, a 20 μ L sample volume was injected 5 times. The chromatograms were monitored by UV at 233nm. The peak area of UV chromatograms were plotted versus the concentration and the calibration curve was constructed using a least square regression equation for the calculation of slope, intercept, and square of correlation coefficient(Table2).

Analysis of Etoricoxib in marketed Tablet Dosage Form

The marketed tablet formulation A (labeled claim: Etoricoxib 90 mg,) and formulation B (labeled claim: Etoricoxib 90 mg) were powdered and powder equivalent to 25 mg of Etoricoxib was weighed. Dissolved in 25 ml methanol. Filtered with whatman filter paper. This final stock solution of formulation A and B are coded as Solution B and C respectively. The standard stock solution of formulation A and B was further diluted with the mobile phase to get the final concentration of about 40 μ g/ml of Etoricoxib.



Validation of method

Precision

Repeatability of sample application and measurement of peak area were carried out using five injections of same sample (40 µg/ml of Etoricoxib). The intra and inter-day variation of the determination of Etoricoxib was carried out at two different concentration levels.

Recovery studies

The analysed samples were spiked with 50, 100 and 150% of the standard Etoricoxib and the mixtures were reanalyzed by proposed method. The experiment was conducted three times. This was done to check for the recovery of the drug at different levels in the formulation.

Stability of Etoricoxib in standard and test solutions

A standard solution was initially prepared (std.no.1) and held under refrigerated condition (4° – 8° c) for up to 30 days and tested against freshly prepared standard solution (std.no.2). A test solution of two different tablets brands were initially prepared (Test 1 and 2) and held under refrigerated condition (4° – 8° c) for up to 30 days and tested against freshly prepared test solution (Test 3 and 4).

RESULTS AND DISCUSSION

Development of the optimum mobile phase

Each mobile phase was filtered through 0.45 µ membrane filter. The mobile phase was allowed to equilibrate phase until steady baseline was obtained. The standard solutions containing Etoricoxib was run and different individual solvents as well as combinations of solvents were tried to get a good separation and stable peak. From the various mobile phases tried, mobile phase containing Methanol (HPLC grade) was selected as it shown sharp peak with symmetry and significant reproducible retention time for Etoricoxib. Chromatogram of Etoricoxib standard drug is shown in Figure 2.

Validation of the method

Precision

The repeatability of sample injection and measurement of peak area were expressed in terms of % RSD and results are depicted in table 3, which revealed intra and inter-day variation of Etoricoxib.

Recovery studies

The proposed method when used for extraction and subsequent estimation of Etoricoxib from marketed formulations after spiking with 50,100 and 150% of additional drug afforded recovery of 99.13-99.52 % as listed in table 4.

Stability of Reserpine in standard and test solutions

Under refrigerated condition (4° – 8° c) standard and test solutions remains stable for up to 30 days (Table 5, 6).

Analysis of Etoricoxib in Marketed Formulations

The Etoricoxib content in marketed formulation A was found to be 98.28 with a %RSD of 0.2403 and in formulation B, 98.79% with a %RSD of 0.3155. It may therefore be inferred that the marketed formulations can be analysed using this

**Gangane et al.**

new and simple method. The low % RSD value indicated the suitability of this method for routine analysis of Etoricoxib in tablet dosage forms.

Limit of Detection and Limit of Quantification

The Limit of Detection (LOD) and Limit of Quantification (LOQ) of the developed method were determined by injecting progressively low concentrations of the standard solutions using the developed HPLC method. The LOD is the smallest concentration of the analyte that gives a measurable response (signal to noise ratio of 3). The LOD for Etoricoxib found to be 0.250. The LOQ is the smallest concentration of the analyte, which gives response that can be accurately quantified (signal to noise ratio of 10). The LOQ was 0.650. It was concluded that the developed method is sensitive.

System Suitability Parameters

System suitability parameters can be defined as tests to ensure that the method can generate results of acceptable accuracy and precision. The requirements for system suitability are usually developed after method development and validation have been completed. The USP (2000) defines parameters that can be used to determine system suitability prior to analysis. The system suitability parameters like Theoretical plates, Resolution (R), Tailing factor (T), LOD (mg/ml), LOQ (mg/ml) were calculated and compared with standard values to ascertain whether the proposed HPLC method for the estimation of Etoricoxib in pharmaceutical formulations was validated or not. The results are recorded in Table-7.

From the optical characteristics of the proposed method it was found that the drug obeys linearity range within the concentration of 20-55 µg/ml. From the results shown precision it was found that the percent RSD is less than 2%, which indicates that the method has good reproducibility. From the results shown in accuracy it was found that the percent recovery values of pure drug from the pre analyzed solutions of formulations were in between 99.13-99.52 %, which indicates that the method is accurate. The system suitability parameters are within the specified limits and which refers the commonly used excipients and additives present in the pharmaceutical formulations did not interfere in the proposed method. The proposed method was found to be simple, precise, accurate and rapid for determination of Etoricoxib from pure and its tablet dosage forms. The mobile phase is simple and economical. The sample recoveries in all formulations were in good agreement with their respective label claims and they suggested noninterference of formulation excipients in the estimation.

CONCLUSION

A convenient and rapid HPLC method has been developed for estimation of Etoricoxib in bulk drug and tablet dosage form. The assay provides a linear response across a wide range of concentrations. Low intra-day and interday % RSD coupled with excellent recoveries. Hence, this method can be easily and conveniently adopted for routine analysis of Etoricoxib in pure form and its dosage forms and can also be used for dissolution or similar studies.

ACKNOWLEDGEMENTS

We are very much thankful to management of Dadasaheb Balpande College of Pharmacy, Nagpur for providing all facilities to carry out this research work.



REFERENCES

1. CIMS 85 April 2004 pg 32,55.
2. COX-2 selective no steroidal anti inflammatory drugs. Do they really offer advantages? *Drugs* 2000 59(6) pg 1207-1216.
3. B. Chauhan, S. Shimpi, A. Paradkar, et al. *AAPS PharmSciTech*, 2005, 6 (3), E402-E412.
4. P. Leclercq, M.G. Malaise, *Rev. Med. Liege.*, 2004, 59, 345.
5. Uma Maheswari R., Sathish Kumar D., Parthiban C., Senivasan P., Krishnaveni A., Alagar Raja M., "The Antiseptic", vol. 101 No. 10 (ii) oct.2004 pg 460-462.
6. Lipsy p. *Am j Med.* 2001 110(3A): IS-5S.
7. Sengupta S. *Ind L Pharmac* 1999 31:322-32
8. Budavari, S., Eds., In; The Merck Index, 12th Edn., merck & Co. Inc, White house Station, NJ, 1994, 691.
9. Reynolds, J.E.F. Eds., In; Martindale, The Extra pharmacopoeia, 30th Edn., The Pharmaceutical press, London, 1993, 1370.
10. Manfred, E.W., In; Burger's Medicinal Chemistry and Drug Discovery, 5th Edn., Vol. III, John Wiley & Sons, Inc., New York, 1995, 490.
11. Kerala State Drug Formulary, Vol.1, Health and Family Welfare Department, Government of Kerala, 1999, 223.
12. Rang H.P., Dale M.M., Ritter J.M., Moore P.K., pharmacology 5th Edition; 432, 2003.
13. Hawkey C, Laine L, Simon T, Neaulieu A, Maldonado – Cocco J, Acevedo E, Shahane A, Quan H, Bolognese J, Mortensen E. 2000. *Arthritis Rheum* 43: 370 –377.
14. Rose M.J., Agarwal N., Woolf E. J.M., Matuszewski B.K, *J.Pharm. Sci.*; 2002, vol. 91, No-2, 405-416.
15. Robert Hartman, ahmed abraham, Andrew Clausen, BingMao, Louis S. Crocker and Zhihong Ge., *Journal of Liquid Chromatography and Related Technologies*, Vol.26, issue 15.
16. S.R.Shahi, G.R. Agrawal, P.B. Rathi, *Rasayan J. Chem* Vol.1, No.2 (2008), 390-394
17. Manish kumar Thimmaraju, Venkat Rao, Hemanth. K, Siddartha.P, HPLC method for the determination of Etoricoxib in bulk and pharmaceutical formulations, *Der Pharmacia Lettre*, Scholars Research Library, 2011: 3 (5) 224-231

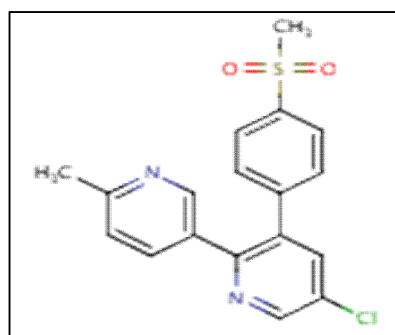


Fig.1.Structure of Etoricoxib.

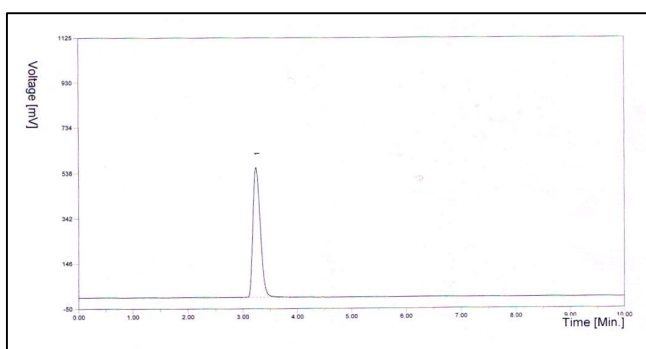


Fig.2.Chromatogram of Etoricoxib standard (40µg/ml).



Gangane et al.

Table 1: Optimized Chromatographic conditions.

Parameters	Method
Stationary phase (column)	LC-10 AT VP Shimadzu Liquid Chromatograph-HPLC with Hyper ODS 2 C18 (size 4.6mmx250mm, particle size 5 µm) column
Mobile Phase	Methanol (HPLC grade)
Flow rate (ml/min)	01 ml/min.
Run time (minutes)	10
Volume of injection loop (µl)	20
Detection wavelength (nm)	233
Drug RT (min)	3.28

Table 2: Linear regression data for the calibration curve.

Parameters	Results
Linearity range (µg/ml)	20-55
Correlation coefficient	0.9998
Slope ± S.D.	0.087 ± 0.54
Y intercept	0

Table 3: Intra and Interday precision of HPLC method.

Sr. No.	Sample No.	% Drug Estimation			
		Interday		Intraday	
		Formulation A	Formulation B	Formulation A	Formulation B
1.	I	98.15	98.42	98.14	98.52
2.	II	98.23	99.81	98.32	98.71
3.	III	98.46	99.13	97.98	97.99
	Mean	98.28	98.79	98.15	98.40
	±S.D.	0.2360	0.3113	0.0040	0.0350
	R.S.D.	0.2403	0.3155	0.0040	0.0355



Gangane et al.

Table 4: Recovery studies.

Formulation A					
Sr. No.	Eq.Wt.of Tablet (g)	Amount of Pure drug added (mg)	Peak area of standard	Peak area of sample	% Recovery*
1	0.025	0.50	105235	108101.87	99.52
2	0.025	1.0	105235	109205.56	99.41
3	0.024	1.5	105235	101058.10	99.32
				Mean	99.41
				±S.D.	0.2472
				R.S.D.	0.2484
Formulation B					
1	0.025	0.5	105235	102645	99.13
2	0.026	1.0	105235	106590	99.42
3	0.025	1.5	105235	103203	99.30
				Mean	99.28
				±S.D.	0.1794
				R.S.D.	0.1799

* Each value is the mean of five observations.

Table 5: Results of Std. solution stability.

Standard no.	1	2
Concentration	40 mcg/ml	40 mcg/ml
Preparation date	04/02/2014	05/03/2014
Mean area	115321	120542
RSD	0.4108	0.5155

Table 6: Results of sample solution stability.

Test no.	1	2	3	4
Concentration	40 mcg/ml	40mcg/ml	40mcg/ml	40 mcg/ml
Preparation date	06/02/2014	06/02/2014	09/03/2014	09/03/2014
Mean Assay	98.19	98.676	97.8566	98.33
RSD	0.2401	0.3153	0.0048	0.0361



Gangane et al.

Table 7: System Suitability Parameters.

Sr.No.	Parameters	Obtained Value
1	Theoretical plates (N)	2450
2	Resolution (R)	2.311
3	Tailing factor (T)	1.4
4	LOD (mg/ml)	0.250
5	LOQ (mg/ml)	0.650



Identification of Binding sites and Calculation of Structural Parameters for ADAM 17 Receptor.

Ramanathan K^{1*}. and S.Kalaiselvan²

¹Department of Bioinformatics, Thanthai Hans Roever College, Perambalur, TamilNadu, India.

²Department of Biotechnology, Thanthai Hans Roever College, Perambalur, TamilNadu, India.

Received: 23 April 2014

Revised: 18 May 2014

Accepted: 28 May 2014

*Address for correspondence

Ramanathan K,
Department of Bioinformatics,
Thanthai Hans Roever College,
Perambalur-621212, TamilNadu, India
E.mail: ramanathanbio@gmail.com.



This is an Open Access Journal / article distributed under the terms of the **Creative Commons Attribution License (CC BY-NC-ND 3.0)** which permits unrestricted use, distribution, and reproduction in any medium, provided the original work is properly cited. All rights reserved.

ABSTRACT

The aim of the work is to focus on the identification of active sites present in the target receptor and calculate the secondary structural parameters. The target receptor sequence was retrieved and calculates the binding sites for the interaction of ligands. It shows the number of binding sites with their locations. We also focused on the structural parameters for the receptor which plays a vital role in biological functions. The composition of Random coils is very high (65.30%) when compared with other parameters. From these observations, it could be possible to understand the interactions with other ligands.

Keywords: Binding Sites, Structural Parameters, Alpha Helix, Beta Sheet, Random Coils, Extended Strand, Ligands.

INTRODUCTION

ADAM 17 was highly expressed in RCC tissues. Compared with blocking γ -secretase, a known mechanism of impairing Notch, blockade of ADAM-17 more effectively down-regulated the expressions of Notch1 and HES-1 receptors. Similarly, we found that the ADAM 17 inhibitor could more efficiently reduce renal cell proliferation and invasive capacity in comparison with the γ -secretase inhibitor DAPT when used at the same dose.[1] Helicobacter pylori are a notorious human and veterinary pathogen responsible for Gastro duodenal cancer due to the epithelial cell signaling mediated by Cytotoxin-Associated Gene A (Cag A). The 3D structure of Cag A is not yet known, such



Ramanathan and Kalaiselvan

information are crucial for understanding the drug binding mechanism and development of novel agonists. Molecular docking was performed to design and optimize new potential drugs against the disease by insilico approach. [2]The target receptor structures were retrieved and predicted the properties using Bioinformatics tools. The receptor Structure was modeled using homologous templates. The receptor structures were also validated by Modeler tool. [3] Hydrogen sulfide treatment significantly increased L-selectin shedding from human neutrophils in an ADAM17dependent manner[4]. Receptor chemical shifts encode detailed structural information that is difficult and computationally costly to describe at a fundamental level. Statistical and machine learning approaches have been used to infer correlations between chemical shifts and secondary structure from experimental chemical shifts[5].Essential to these successes has been the use of innovative strategies for finding binding modes that are achievable, that is, identifying binding partners and docked conformations that can be successfully stabilized via sequence optimization and backbone refinement [6]. Conventional platinum coils because imaging artifacts that reduce imaging quality and therefore impair imaging interpretation on intraprocedural or noninvasive follow-up imaging [7].Computational searches for novel ligands for a given receptor binding site have become ubiquitous in the pharmaceutical industry, and are potentially equally useful in helping identify small-molecule tools for biology[8]. A combination of receptor-ligand docking and ligand-based QSAR approaches has been elaborated, aiming to speed-up the process of virtual screening. In particular, this approach utilizes docking scores generated for already processed compounds to build predictive QSAR models that in turn assess hypothetical target binding affinities for yet undocked entries[9].

METHODOLOGY

The Receptor ADAM 17 is responsible for cancer and the sequence for ADAM 17 was retrieved from NCBI database and subjected to PROSITE tool for the identification of binding sites. It shows the number of binding sites which is present in ADAM 17 and the sequence was submitted to SOPMA tool. The Secondary Structural parameters such as α -helix, β -sheet, Turns, Coils, Random and Extended strand were calculated.

RESULTS AND DISCUSSION

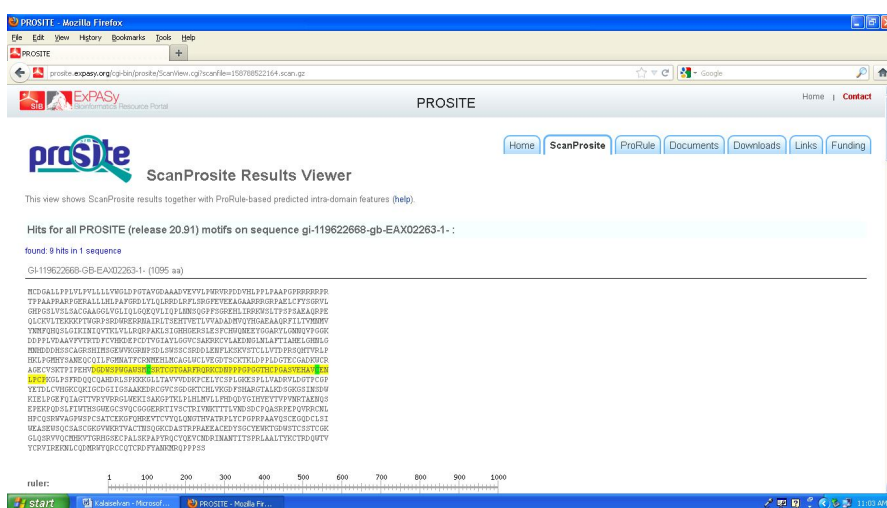


Fig 1: ADAM 17 sequence submitted to Prosite tool.



Ramanathan and Kalaiselvan

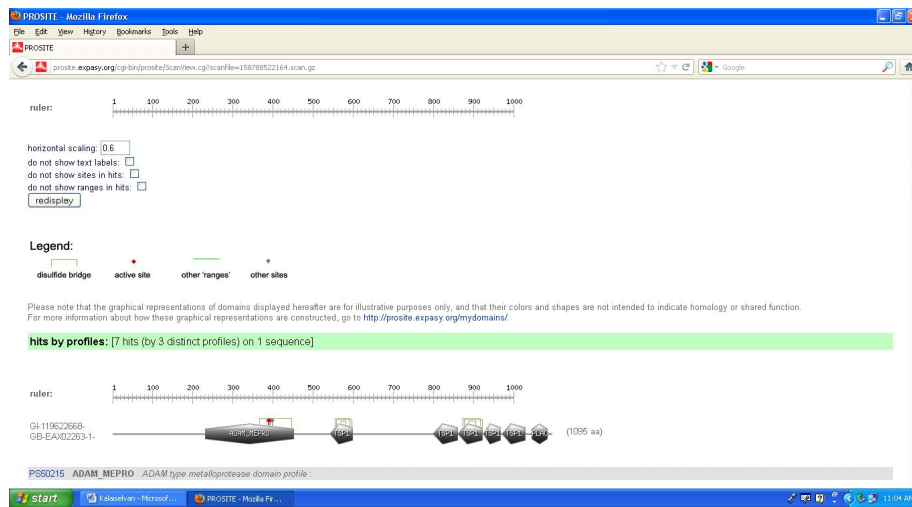


Fig 2: Prosite tool shows 9 hits in the sequence

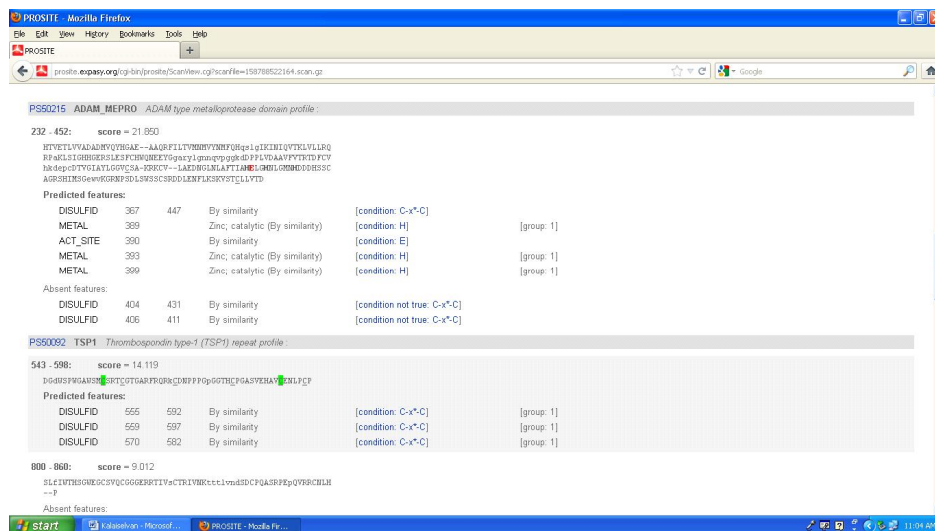


Fig 3: Identification of Binding Sites with their positions.

Table 1: Identification of Binding Site by Prosite Tool

No. of Binding Sites	Position of Binding Sites
1	232 - 452
2	543 - 598
3	800 - 860
4	861 - 922
5	925 - 968
6	972 - 1029
7	1045 - 1089
8	386 - 359
9	984 - 1007



Ramanathan and Kalaiselvan

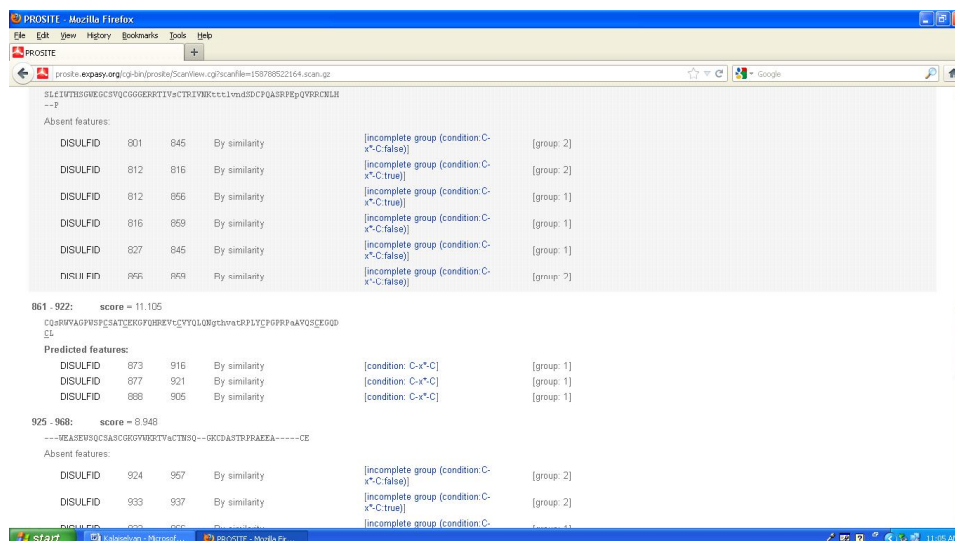


Fig 4: Disulphide Bridges in ADAM 17

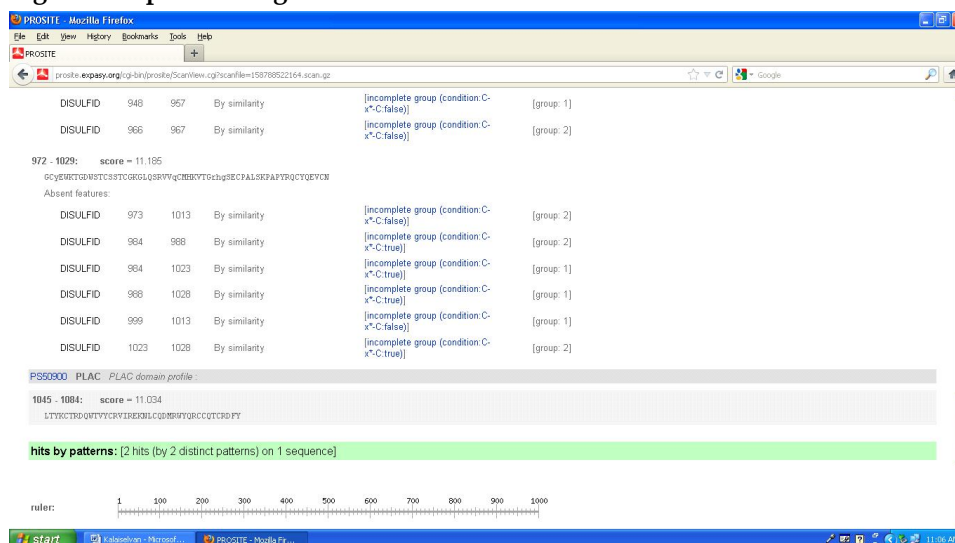


Fig 5: Location of Disulphide Bridges

Table 2: Analysis of Secondary Structural Parameters in ADAM 17

S.No	2° Structure Parameters	Composition in %
1	Alpha Helix	14.52
2	Extended Strands	16.71
3	Beta Sheet	3.47
4	Random Coil	65.30



Ramanathan and Kalaiselvan

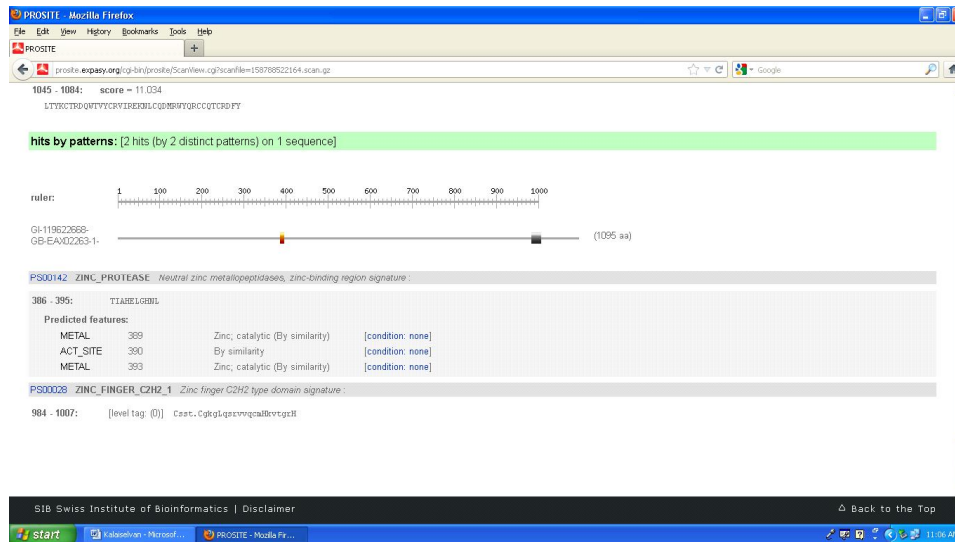


Fig 6: Identification of Metal Binding Sites

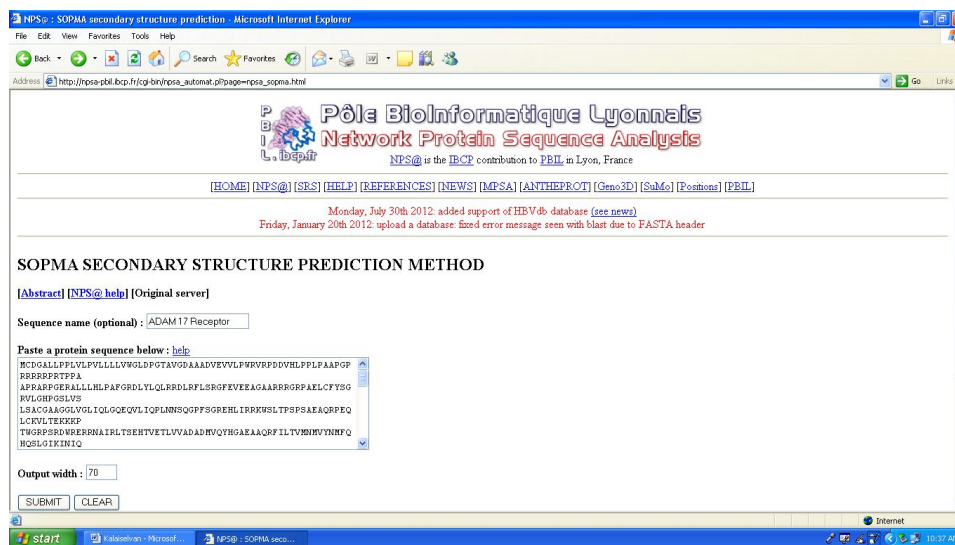


Fig 7: Submission of ADAM 17 Sequences to the SOPMA Tool

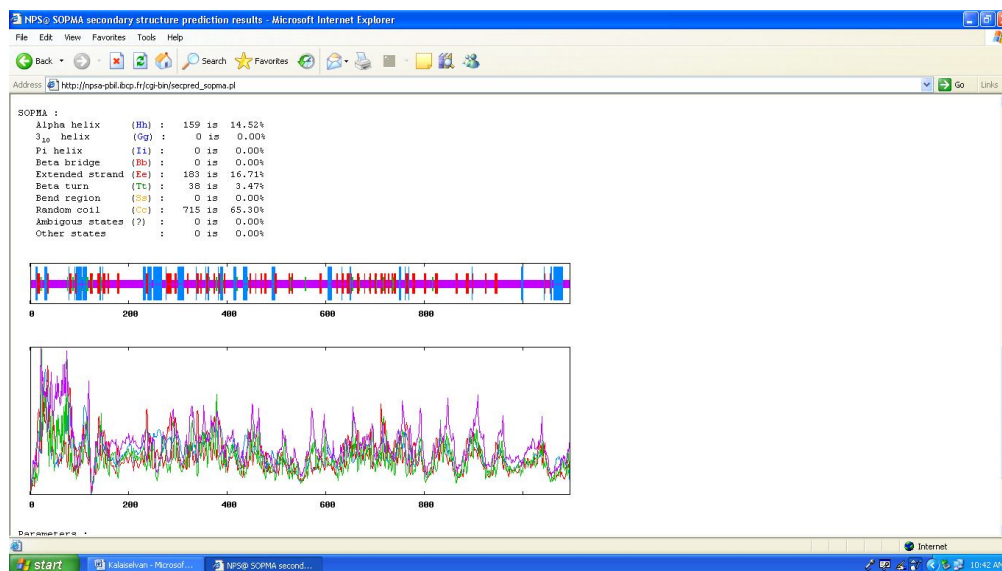


Fig 10: Composition of Structural Parameters in ADAM 17

The ADAM 17 which is an important target receptor and it is responsible for cancer. So, we are highly focused and calculated the number of binding sites with their locations. The ADAM 17 sequence was retrieved and submitted to Prosite tool (Fig 1). Fig 2 shows that the binding sites of the receptor were calculated. The number and position of the binding sites was calculated and showed in Fig 3, 4, 5 and 6 respectively. Table 1 which represents the positions of binding sites. The position of the first binding site is from 232 to 452, the second binding site occurs between 543 and 598, third binding site is between 800 and 860. The position for fourth and fifth binding site occurs from 861 to 922 and 925 to 968 respectively. The sixth binding site occurs between 972 and 1029, and the position of seventh binding site is from 1045 to 1084. The target receptor sequence was submitted to SOPMA tool (Fig 7). Fig 8 which represents the secondary structural parameters for the target receptor. The composition of secondary structural parameters was displayed in Fig 9 and Fig 10 respectively. Table 2 which represent the composition of each secondary structural parameter such as *alpha* Helix (14.52%), extended strands (16.71%), *beta* Sheet (3.47%) and Random Coils (65.30%).

CONCLUSION

The ADAM 17 is responsible for cancer and it plays a significant role in all biological functions. There are number of ligands are ready to bind with the receptor and address the problems for cancer. The target receptor which shows 9 active sites and the secondary structural parameters were also calculated. The composition of Random coil is very high (65.30%) when compared with other parameters. The alpha helix, extended strands and beta sheet are also present at the moderate level. From these observations, we found that the target receptor may be binds with the number of ligands which act as an antitumour agent. Our study concluded that plant alkaloids such as Vinblastin, Vincristin and n-hexa decanoic acid act as a ligand and it shows better binding energy with the target receptor.



REFERENCES

1. Guo Z, Jin X, Jia H. (2013) Inhibition of ADAM-17 more effectively down-regulates the Notch pathway than that of γ -secretase in renal carcinoma. *J Exp Clin Cancer Res.* 32:26.
2. Sinosh Skariyachan, Ashwini MP, Ambreen Hina CH, Diksha M Jain , Abhilash M (2010). Design and discovery of novel therapeutic drugs against *Helicobacter pylori* gastro duodenal cancer by Insilico approach. *Research Journal of Pharmaceutical, Biological and Chemical Sciences* 1(4) :1005 - 1007
3. Ramachandran M and Elumalai EK (2012). Novel drug target identification on UDP Glucose 4-epimerase enzyme in *Catharanthus roseus* by insilico model. *Asian Pacific Journal of Tropical Biomedicine* S1047-S1051.
4. Ball CJ, Reiffel AJ, Chintalapani S, Kim M, Spector JA, King MR. (2013) Hydrogen sulfide reduces neutrophil recruitment in hind-limb ischemia-reperfusion injury in an L-selectin and ADAM 17-dependent manner. *Plast Reconstr Surg.* 131(3):487 - 497
5. Mechelke M, Habeck M.A (2013) Probabilistic model for secondary structure prediction from receptor chemical shifts. *Receptors.* 81(6):974-983
6. Der BS, Kuhlman B. (2013) Strategies to control the binding mode of de novo designed receptor interactions. *Curr Opin Struct Biol.* 35(6): 1023 – 1034.
7. Mordasini P, Kraehenbuehl AK, Byrne JV, Vandenberghe S, Reinert M, Hoppe H, Gralla J. (2013) In Vitro and In Vivo Imaging Characteristics Assessment of Polymeric Coils Compared with Standard Platinum Coils for the Treatment of Intracranial Aneurysms. *AJNR Am J Neuroradiol.* 81(6):984-993
8. Pitt WR, Calmiano MD, Kroeplien B, Taylor RD, Turner JP, King MA. (2013). Structure-based virtual screening for novel ligands. *Methods Mol Biol.* 1008:501-19
9. Cherkasov A, Ban F, Li Y, Fallahi M, Hammond GL. (2006) Progressive docking: a hybrid QSAR docking approach for accelerating in silico high through out screening. *Journal of Med Chem.,* 14; 49 (25):7466-78.



Use of *Cocculus hirsutus* (L.) Diels Fruit Extract as a Natural Indicator in Acid Base Titration.

Smita Mujbaile*, Kamlesh Niranjane, Bhushan Pahune and Sandhya Bagde

Department of Pharmaceutical chemistry, Dadasaheb Balpande College of Pharmacy, Besa, Nagpur-440034 (M.S.) India.

Received: 20 May 2014

Revised: 25 May 2014

Accepted: 28 May 2014

*Address for correspondence

Smita G. Mujbaile,
Assistant Professor, Department of Pharmaceutical chemistry,
Dadasaheb Balpande College of Pharmacy,
Besa, Nagpur-440034 (M.S.) India.
E.mail: smitamujbaile@gmail.com.



This is an Open Access Journal / article distributed under the terms of the **Creative Commons Attribution License** (CC BY-NC-ND 3.0) which permits unrestricted use, distribution, and reproduction in any medium, provided the original work is properly cited. All rights reserved.

ABSTRACT

In present scenario natural indicators are more widely prepared as it has several advantages over synthetic one. Mostly flower extracts are used for the preparation of natural indicators but most of the part of the plant contains anthocyanin which is responsible for the development of colour, hence fruit parts are also used for the preparation of natural indicator. In this research work fruit part of *Cocculus hirsutus* is used as natural indicator, it contains six anthocyanins like cyanidin, pelargonidin, malvidin, delphinidin, petunidin and peonidin. *Cocculus hirsutus* is a species of the *Cocculus* genus, belonging to the family Menispermaceae. The present work highlights the use of *Cocculus hirsutus* fruit extract as an acid base indicator in different types of acid base titrations. The equivalence points obtained by the fruit extract coincident with the equivalence points obtained by standard indicators. In case of weak acid and weak base titration, the results obtained by the fruit extract matched with the results obtained by mixed indicator. This natural indicator was found to be a very useful, economical, simple and accurate for the said titration.

Key words: *Cocculus hirsutus*, Acid base indicator, Natural indicator, Anthocyanin.

INTRODUCTION

Cocculus hirsutus (L.) Diels belonging to family menispermaceae is a perennial climber mainly found in tropical and subtropical climatic condition [1]. *Cocculus hirsutus* has various synonyms in ayurvedic texts like sreyasi, sthapani, pracina, rasa, papaveli, vanatiktaka, patha, ambastha, viddhakami etc. and commonly known as broom creeper, ink berry, huyer (Bengali), farid buti (Hindi, Urdu), daagadi balli, daagadi soppu and kaage maari (Kannada), vasanvel

**Smita Mujbaile et al.**

(Konkani), paathalagarudakkoti and paathaalamuuli (Malayalam), vasanvel (Marathi), musakani (Oriya), farid buti and wallur (Punjabi), ambastha, dirghakanda, dirghavalli, garudi, mahamula, patalagarudi, pracina, sauparni, somavalli, sreyasi, sthapani, vanatiktaka, vatsadani, viddhakarni (Sanskrit), kattu-k-koti (Tamil), chipuru-tiga, dusaritiga, katlatige (Telugu)[2]. *Cocculus hirsutus* is widely found in many parts of world throughout tropical and subtropical regions like in Sudan, central Asia, China and India. The plant grows all over India, especially in dry regions. The plant is a climber with green flowers bloom in February –March and fruits in May- June. In some places it is found along with water stream, hedges. Tribals of Jhabua, Khargone and Dhar use the fruit of *Cocculus hirsutus* to cure Jaundice [3]. It contains triterpenoid hirsudiol [4], Alkaloids cohirsinine and Jamtinine [5, 6]. Seeds are curved and fleshy with annular embryo. Leaves are simple, alternate, ovate, sub deltoid or three lobed, obtuse and mucronate. The base of leaf is subcordate or truncate. Petioles are very short, dark green, usually subauriculate at the base. The fruit is a drupe which is size of small pea with dark purple endocarp (Fig.1a and b). The flowers are very small, unisexual and green. The male flowers occur in axillary cymose panicles, stamens are six, free, embraced by the petals, anthers are subglobose in shape. Female flowers are in axillary clusters of 1-3 and staminoids are six and styles usually cylindrical [7, 8, 9].

Anthocyanins present in plant parts are responsible for the development of colour. Anthocyanins are water soluble pigment belonging to family of flavonoids. They are responsible for purple, blue, red and orange colours of several fruits and flowers. Mostly six anthocyanidins are present in fruits and vegetables namely cyanidin, pelargonidin, malvidin, delphinidin, petunidin and peonidin. The anthocyanin content and compositions are different in pigmented fruits depending on the varieties and origin [10]. The roots, fruits and leaves of *Cocculus hirsutus* have great medicinal value and are used both, internally as well as externally for medicinal purpose. The plant is in local area people used as tonic but there is paucity of data available on immunomodulatory activity of *Cocculus hirsutus* in normal animals [11]. The leaves are cooling, mucilaginous and are useful in eczema. Internally, it is useful in various diseases. *Cocculus hirsutus* has mild laxative, digesting and appetite stimulant properties. It is used in anorexia, with great benefit. It also works well in asthma, cough and cold. In premature ejaculation *Cocculus hirsutus* has extremely good results in delaying the ejaculation. The juice of leaves, being diuretic, is salutary in burning micturition and strangury. The roots are useful in serpent bite; also, the roots have digestive, carminative, demulcent, depurative, emollient, tonic and antipyretic properties. Along with poisonous bites, they are useful in leprosy, skin diseases, pruritus, dyspepsia, colic, flatulence, bronchitis, cough, gout, intermittent fever, tubercular glands, hypertension and general debility [12-18]. Therefore present work aims at studying extract of *Cocculus hirsutus* as an indicator. Present investigations were carried out to justify its uses in the indigenous system of medicine and in analysis as a natural indicator.

MATERIALS AND METHODS

Plant Material

The fruit of *Cocculus hirsutus* were collected from Kanhapur village, Wardha (M.H.) in the month of March-April. Its identity was confirmed from the department of Botany, RTM Nagpur University, Nagpur. The collected fruits were dried in shade and stored.

Solvent Extraction

Cocculus hirsutus (L.) Diels fruits (Fig. a and b) were washed and dried. Then 2 gm fruits were extracted by crushing with water. The extract was stirred with a glass rod to complete extraction. The extract was centrifuged (3000 rpm/min) at room temperature for 15 minutes. The supernatant (Fig. 1c) was separated and filtered. Finally extract was filtered and used as indicator in several acid base titrations. The experimental work was carried out by using the same set of glassware for all type of titrations. As the same aliquots were used for both titrations i.e. titration by using standard indicator and fruits extract. The equimolar titrations were performed using 25 ml of titrant with three drops



Smita Mujbaile et al.

of indicator. All the parameters for experiment are given in Table 1. A set of five experiments was carried out. The mean and standard deviation were calculated from results and also the solvent extracts were concentrated under reduced pressure and preserved at 5°C in airtight bottle.

RESULTS AND DISCUSSION

The prepared fruit extract was screened for its use as an acid base indicator in various acid base titrations, and result of screening compared with the result obtained by standard indicators like methyl red, phenolphthalein and mixed indicator [methyl orange: bromocresol green (1:2)] for strong acid v/s strong base (HCl and NaOH), strong acid v/s weak base (HCl and NH₄OH), weak acid v/s weak base (oxalic acid and NH₄OH) titrations respectively [19,20]. All these parameters are shown in Table 1. For all titrations the equivalence points obtained by the fruit extract matched with the equivalence points obtained by standard indicators. The results of screening were listed in Table 2.

CONCLUSION

It is concluded from the data, the present research work of the *Cocculus hirsutus* fruit extract alone can serve the purpose of indicator in weak acid and weak base titration, where generally mixed indicators employed. Another benefit of this titration is that it gives colored end point at the equivalence point. The results obtained in all types of acid base titrations lead us to conclude that it was due to the presence of flavonoids and anthocyanins sharp color changes occurred at the end point of the titrations. At last we can say that it is always beneficial to use *Cocculus hirsutus* fruit extract as an indicator in all types of acid base titrations because of its cost effectiveness, simplicity and availability.

ACKNOWLEDGEMENTS

The authors are very much thankful to Mr. Manoj V. Balpande President and Dr. U.N. Mahajan Principal of Dadasaheb Balpande College of Pharmacy, Besa Nagpur for providing the necessary facilities to carry out the research work. The authors are also grateful to Department of Botany, R.T.M. Nagpur University, Nagpur, India.

REFERENCES

1. Mandarin KM. Indian Material Medica, Vol. I, Popular Prakashan, New Delhi, 1976. ; 362.
2. www.flowersofindia.net/catalog/slides/Broom%20Creeper.html
3. Samvatsar S. and Diwanji NB. Plant sources for the treatment of jaundice in the tribals of western Madhya Pradesh of India. J Ethnopharmacol 2000 ; 73: 313-316.
4. Ahmad VU, Mohmmad FV and Rasheed T. Hirsudiol, A Triterpenoid from *Cocculus hirsutus*. Phytochem 1987; 26:793.
5. Ahmad VU, Rasheed T. and Iqbal S. Cohirsinine, an alkaloid from *Cocculus hirsutus*. Phytochem 1991; 30:1350.
6. Ahmad VU and Iqbal S. Jamtinine, an alkaloid from *Cocculus hirsutus*. Phytochem. 1993; 33:35.
7. *The Wealth of India* — A Dictionary of Indian, Raw Materials, Vol. 2, Publications and Information Directorate, CSIR, New Delhi; 1950: 35-36.
8. Shah GL, Flora of Gujarat, vol.1.Ragistrar, 1st edition, S.P.university, V V.nagar; 1978:52-54.
9. Chopra RN, Chopra IC, Handa KL, et al. Indigenous Drugs of India, U.N.Dhur & Sons Pvt Ltd., Calcutta; 1958:501.
10. Oh YS, Lee JH, Yoon SH, Oh CH, Choi DS, Choe E, Jung MJ, J. Food sci.2008;73:378-389
11. Rastogi B, Tiwari U, Dubey A, Bawara B, Chauhan NS and Saraf DK. Immunostimulant activity of *cocculus hirsutus* on immunosuppressed rat. Pharmacologyonline. 2008; 3: 38-57.



Smita Mujbaile et al.

12. Chopra RN, Nayar SL, Chopra IC, Glossary of Indian Medicinal Plants, National Institute of Science Communication, New Delhi; 1996:72.
13. Caius JE. The medicinal and poisonous plants of India, Jodhpur, scientific publishers; 1986: 166-171.
14. Chadha YR, The Wealth of India- A dictionary of Indian Raw Materials and industrial products. CSIR, New Delhi; 1950: 258.
15. Maasilamani G, Shokat A, J. Res. in Ayurveda and Siddha; 1981(2): 109.
16. Nandkarni KM, Indian Materia Medica, Vol. I, Popular Prakashan, New Delhi; 1976:362.
17. Guhabakshi DN, Flora of Murshidabad, West Bengal, India, Scientific publisher; 1984:47.
18. Chatterjee TK, Herbal Options, 1st ed. M/s Eastern Traders, Calcutta; 1996:157-178.
19. Kasture AV, Mahadik KR, Wadodkar SG, More HN. Pharmaceutical Analysis, Nirali Prakashan, Pune:2007;(1):pp.6.11-6.12.
20. http://en.Wikipedia.org/wiki/PH_indicator. Accessed – December 10, 2007.

Table 1: Analyzed parameters and the comparison of color change.

Titrate	Titrant	Indicator Colour Change	
		Standard (pH range)	Fruit Extract (pH range)
HCl	NaOH	Red to Yellow (3.2-11.67)	Pink to Green (2.8-10.45)
HCl	NH ₄ OH	Colorless to Pink (3.2-8.2)	Pink to Faint green (2.8-9.20)
Oxalic acid	NaOH	Red to Yellow (4.7-9.2)	Pink to Green (1.96-9.80)
Oxalic acid	NH ₄ OH	Orange to Blue-green (4.7-7.8)	Pink to Faint green (1.96-7.90)

HCl: - Hydrochloric acid, NaOH:-Sodium Hydroxide, NH₄OH:-Ammonium Hydroxide



Fig.1.(a) The fruits of *Cocculus hirsutus* with leaves; (b) Collected fruits of *Cocculus hirsutus* (c) The extract of fruits of *Cocculus hirsutus*.



Smita Mujbaile et al.

Table 2: Screening results of various titrations.

Sr. No.	Titration (Titrant v/s Titrant)	Strength (Moles)	Indicator	Readings with S.D. (+/-)
1	NaOH V/S HCl	0.1	Methyl red	12.4±1.13
			Fruit extract	12.7±1.17
		0.5	Methyl red	12.8±1.19
			Fruit extract	12.6±1.14
		1	Methyl red	12.9±1.20
			Fruit extract	12.9±1.21
2	NH ₄ OH V/S HCl	0.1	Phenolphthalein	10.8±1.13
			Fruit extract	10.6±1.11
		0.5	Phenolphthalein	09.9±1.11
			Fruit extract	10.1±1.20
		1	Phenolphthalein	10.4±1.18
			Fruit extract	10.2±1.13
3	NaOH V/S Oxalic Acid	0.1	Methyl red	15.01±1.22
			Fruit extract	15.7±1.26
		0.5	Methyl red	15.8±1.29
			Fruit extract	15.9±1.31
		1	Methyl red	15.4±1.28
			Fruit extract	15.3±1.26
4	NH ₄ OH V/S Oxalic Acid	0.1	Mixed indicator	09.8±1.23
			Fruit extract	09.6±1.15
		0.5	Mixed indicator	09.4±1.16
			Fruit extract	09.8±1.18
		1	Mixed indicator	09.5±1.16
			Fruit extract	09.5±1.11

HCl: Hydrochloric acid, NaOH: Sodium hydroxide, NH₄OH: Ammonium hydroxide.



Modeling the Distribution of Iran Life Zones Using CCA.

Mohammad Mousaei Sanjerehei

Department of Plant Protection, Yazd Branch, Islamic Azad University, Yazd, Iran

Received: 22 April 2014

Revised: 20 May 2014

Accepted: 28 May 2014

*Address for correspondence

Mohammad Mousaei Sanjerehei,
Department of Plant Protection,
Yazd Branch, Islamic Azad University,
Yazd, Iran.
E.mail: mmusaei@iauyazd.ac.ir



This is an Open Access Journal / article distributed under the terms of the **Creative Commons Attribution License** (CC BY-NC-ND 3.0) which permits unrestricted use, distribution, and reproduction in any medium, provided the original work is properly cited. All rights reserved.

ABSTRACT

Distribution of the life zones of Iran including Hyrcanian humid forest, Zagros semiarid and humid forest, humid grassland, semiarid scrub-grassland, arid desert scrub and arid desert life zones was predicted using canonical correspondence analysis (CCA). The environmental predictors used for modeling were elevation (E), mean annual precipitation (P) and temperature (Tmean), maximum (Tmax) and minimum temperature (Tmin), relative humidity (H), and reference evapotranspiration (ETo). The predicted potential distribution map of the life zones was compared to the reference map using kappa coefficient and Z statistic to obtain the level of accuracy. P was the most important factor in the distribution of the life zones followed by H, E, ETo, Tmean, Tmax and Tmin. The highest accuracy of predicted distribution was related to the Hyrcanian humid forest and arid desert life zones. Continuously distributed life zones with no gap had the most accurate predicted distribution, while the life zones which were discontinuously and sparsely distributed had the lowest accurate predicted distribution. The Hyrcanian humid forest life zone, the dense forest of Iran, was found to be distributed in the regions with high precipitation where mean temperature increases with increasing minimum temperature but decreasing maximum temperature. Although CCA could distinguish between the life zones, the overlap between the predicted distributions of life zones indicated that CCA cannot efficiently model and delimit the life zones which have approximately similar environmental conditions. Instead, CCA enables to efficiently distinguish and delimit the life zones with very humid and very arid climate.

Keywords: canonical correspondence analysis, distribution, life zones, evapotranspiration.



Mohammad Mousaei Sanjerehei

INTRODUCTION

Advances in distribution modeling of species and life zones enable us to potentially evaluate the relationships between environmental variables and vegetation attributes such as distribution of species and communities [9], species composition [16], forecast biodiversity patterns at different spatial scales [24], determine the potential of an area to support a particular species and assess the influence of climate changes and management strategies on vegetation types during successional stages. The study of life zones in large scales considers multiple components of ecosystems and their interactions. Species and life zone distribution over a large scale is mainly controlled by climatic factors such as temperature, precipitation and evapotranspiration [10, 13], whereas patchy distribution over a smaller area is likely to result from more detailed factors such as micro-topographic [17] and soil properties [13]. The vegetation distribution models are based on quantifying vegetation-environment relations. In such models both presence-absence and abundance data can be applied. A variety of quantitative world and regional models have been presented to relate the environmental variables to distribution of life zones [13, 2], plant biodiversity [28], plant species [18, 7] and plant communities [25]. Canonical Correspondence Analysis (CCA) [20] is one of the most efficiently used methods for modeling environment-vegetation relations such as predictive mapping of forest composition and structure [16] and modeling distribution of plant species [11, 3]. CCA is unique among the ordination methods in that the ordination of the main matrix representing species data (by reciprocal averaging) is constrained by a multiple regression on environmental variables included in the second matrix. CCA is most likely to be useful when species responses are unimodal (hump-shaped). In this analysis main axes of a correspondence analysis are constrained to be a linear combination of environmental variables [12]. CCA is appropriate for data set with many zeros (i.e. presence-absence data) [11]. It is implicitly based on the chi-squared distance measure where samples are weighted according to their totals [15]. Predictive map of life zone distribution can be produced using CCA and GIS. A regression equation can be made based on the canonical coefficients of the environmental predictors of the canonical

MATERIALS AND METHODS

The data layers used for modeling the distribution of Iran life zones were digital elevation model (DEM), mean annual temperature (Tmean), mean annual maximum temperature (Tmax) mean annual minimum temperature (Tmin), mean annual precipitation (P), mean annual relative humidity (H) and mean annual reference evapotranspiration (ETo) (Fig 1). DEM, P and Tmean layers were created respectively, using interpolating contour maps of elevation, precipitation and mean annual temperature of Iran, produced by National Cartographic Center of Iran (NCCI). The data of 180 synoptic stations throughout Iran from 1955-2005 were applied to produce point layers of Tmax, Tmin, H and ETo. The point maps were interpolated using kriging algorithm. Reference evapotranspiration was determined using Penman-Monteith equation [1] based on the data of elevation, latitude, mean annual temperature, maximum and minimum temperature, relative humidity, wind speed and sunshine hours of the synoptic stations.

$$ET_o = \frac{0.408 \Delta (R_n - G) + \gamma \frac{900}{T + 273} U_2 (e_s - e_a)}{\Delta + \gamma (1 + 0.34 U_2)}$$

where ETo : reference evapotranspiration [mm day⁻¹], Rn: net radiation at the crop surface [MJ m⁻² day⁻¹], G: soil heat flux density [MJ m⁻² day⁻¹], T :mean air temperature [°C], U₂: wind speed at 2 m height [m s⁻¹], e_s: saturation vapour pressure [kPa], e_a :actual vapour pressure [kPa], e_s - e_a: saturation vapour pressure deficit [kPa], Δ :slope vapour pressure curve [kPa °C⁻¹] and γ : psychrometric constant [kPa °C⁻¹].



Mohammad Mousaei Sanjerehei

The values of the produced raster map for each environmental variable were standardized by calculating z scores as $(x - \bar{x} / \delta)$. To predict the potential distribution of the life zones of Iran using CCA, all data layers and the reference life zone map of Iran (produced by NCCI) (Fig 2) were displayed together on one map window in ILWIS. 30 points were selected approximately uniformly on each life zone (a total of 180 points), and the elevation, mean, maximum, and minimum temperature, precipitation, humidity and reference evapotranspiration values for each point were registered. Two matrices were constructed in CCA. In the main matrix, presence/absence data of life zones were used, and the second matrix was composed of the values of environmental variables. The map of environmental gradient for each canonical axis was produced using the regression equation based on the canonical coefficients using the four first axes. To predict the potential distribution of each life zone, Euclidean distance to the centroid of each life zone in canonical space was calculated as

$$d(p, q) = \sqrt{(p_1 - q_1)^2 + (p_2 - q_2)^2 + \dots + (p_n - q_n)^2}$$

The centroid (weighted average) of a life zone indicates the position of the life zone' distribution along an environmental variable [21]. The weighted average of each life zone (u_k) with respect to any gradient x (ordination axis) was calculated as [22]:

$$u_k = \sum_{i=1}^n \frac{y_{ik}}{y_{+k}} x_i$$

with y_{ik} : the presence (1) / absence (0) of the life zone k in sample point i ($i=1...180$), ($k=1... 6$). x_i : the value of gradient x at sample point i , and y_{+k} : the sum of the presence of life zone k in all sample points. The weighted average (centroid) for presence-absence data is simply the mean of the ordination axis values over the sampling points selected for each life zone [19]. The distribution range of each life zone was predicted based on the weighted standard deviation (tolerance) of each life zone. The weighted standard deviation (tolerance) of each life zone is

$$t_k = \sqrt{\sum_{i=1}^n \frac{y_{ik}}{y_{+k}} (x_i - u_k)^2}$$

For a fair statistical comparison of life zone tolerance, $y_{+k} (1 - 1 / N_2)$ was used instead of y_{+k} in the t_k equation to remove the bias and prevent the underestimation of the true tolerance.

$$N_2 = \left[\sum_{i=1}^n \left(\frac{y_{ik}}{y_{+k}} \right)^2 \right]^{-1}$$

where N_2 is the effective number of occurrences of life zone k [22]. For presence-absence data, the tolerance is the standard deviation (δ_{n-1}) of the values of the ordination axis over the sampling points selected for each life zone [21]. Because 6 main life zones of Iran were studied in this research, the predicted map was compared to the reference map following separating the other land covers (agricultural lands, dry farmlands, saltlands, wetlands, water and rock). To obtain the accuracy of the prediction, Kappa coefficient was calculated to compare the predicted maps with the reference map. Kappa coefficient was calculated as:



Mohammad Mousaei Sanjerehei

$$Kappa = \frac{N \sum_{i=1}^k x_{ii} - \sum_{i=1}^r (x_{i+} \times x_{+i})}{N^2 - \sum_{i=1}^r (x_{i+} \times x_{+i})}$$

where r is the number of rows in the matrix, x_{i+} and x_{+i} are the marginal totals of row i and column i respectively. N is the total number of observations and x_{ii} is the number of observations in rows i and column i . Kappa statistic strength of agreement is classified as: <0 poor, 0-0.20 slight, 0.21-0.40 fair, 0.41-0.60 moderate, 0.61-0.80 substantial and 0.81-1 almost perfect [14]. To test the significance of Kappa coefficient, Z statistics was calculated [5].

$$z = \frac{k}{\sqrt{\text{var}(k)}}$$

The value of $z > 1.96$ ($\alpha = 0.05$) indicates that the classification is significantly better than a random result.

$$\text{var}(k) = \frac{1}{N} \left[\frac{\theta_1(1-\theta_1)}{(1-\theta_2)^2} + \frac{2(1-\theta_1)(2\theta_1\theta_2 - \theta_3)}{(1-\theta_2)^3} + \frac{(1-\theta_1)^2(\theta_4 - 4\theta_2^2)}{(1-\theta_2)^4} \right]$$

where $\theta_1 = 1/N \sum_{i=1}^C x_{ii}$, $\theta_2 = 1/N^2 \sum_{i=1}^C x_{i+} + x_{+i}$, $\theta_3 = 1/N^2 \sum_{i=1}^C x_{ii}(x_{i+} + x_{+i})$,

$$\theta_4 = 1/N^3 \sum_{i=1}^C \sum_{j=1}^C x_{ij}(x_{j+} + x_{+i})^2$$

To evaluate the efficiency of CCA in modeling and delimiting the life zones, overlap between the life zones was determined using kappa coefficient. The kappa value of equal to 1 indicates maximum overlap between two life zones.

RESULTS

CCA analysis

Distribution of the life zones of Iran was predicted based on 7 environmental variables using CCA. The ordination biplots for the life zones of Iran (Fig 3) indicates the overall results of CCA ordination. Overall the CCA explained 32.3% of the variance in life zone presence-absence (table 1). Axis 1 and 2 explained 15.7% and 10.8% of the variability in life zone data respectively (26.5% out of 32.3%). All the 7 environmental predictors had the highest correlation with these two axes. P, H, ETo and Tmax had the highest correlation with the first axis, and E, Tmean and Tmin had the highest correlation with the second axis (table 2). Therefore, these two axes were used to show CCA biplots of life zones and to interpret the life zone-environment relations. The life zone-environment correlation was 0.885, 0.735, 0.465 and 0.277 for the axis 1, 2, 3 and 4 respectively. Canonical coefficients, t- values and correlation of each environmental predictor with CCA axes are presented in table 2. Axis 1 (Eigenvalue = 0.783) is dominated by precipitation (P), humidity (H), evapotranspiration (ETo) and maximum temperature (Tmax) and is interpreted as a gradient of increasing P and H and decreasing ETo and Tmax from arid desert to the Hyrcanian humid forest life



Mohammad Mousaei Sanjerehei

zone (Fig 3). P had the highest correlation with the first axis. All life zones were sorted out well along these gradients except the Zagros semiarid and humid forest and humid grassland life zones which had the same score on axis 1. This indicates that P, H, ETo and Tmax cannot differentiate between these two life zones. The Hyrcanian humid forest life zone was indicated by the highest amount of P and H and lowest amount of ETo and Tmax followed by Zagros semiarid and humid forest and humid grassland life zones. Arid desert is the life zone with the lowest amount of P and H and highest amount of Tmax and ETo followed by arid desert scrub life zone. Semiarid scrub-grassland life zone is dominant at middle P, ETo Tmax and H. Axis 2 (Eigenvalue = 0.54) is dominated by elevation (E), mean temperature (Tmean) and minimum temperature (Tmin) among which E has the highest correlation with this axis. The high score of Hyrcanian humid forest on axis 2 indicated that this life zone is found on the lowest elevation. Arid desert life zone is also a low elevation life zone. Humid grassland life zone on axis 2 exhibited a preference for a high E and low Tmean and Tmin followed by semiarid scrub-grassland life zone. The axis2 score of close to zero for Zagros semiarid and humid forest life zone showed that this life zone is found on mid elevation with a moderate Tmean and Tmin. Arid desert scrub life zone on axis 2 exhibits a slight preference for locating at higher E, Tmean and Tmin (Fig 3). Figure 4 shows the potential distribution map of Iran life zones produced based on the canonical (regression) coefficients of the four first axes of CCA, the centroid and the tolerance of each life zone.

Accuracy of the predicted distribution

The calculated kappa values indicated that the highest accuracy of prediction was related to the Hyrcanian humid forest (kappa = 0.57) and arid desert (kappa = 0.51) life zones. A moderate agreement was found between the predicted distribution of these two life zones and the reference data (table 3). There was a fair agreement on semiarid scrub- grassland, Zagros semiarid and humid forest (kappa = 0.22) and arid desert scrub (kappa = 0.21) life zones. A slight agreement (kappa = 0.16) was found between the distribution of humid grassland life zone and the reference data.

Overlap between the distribution of life zones

The kappa value between the life zones (table 4) showed the largest overlap between the predicted distribution of humid grassland and the Zagros semiarid and humid forest life zones followed by humid grassland and semiarid scrub-grassland, semiarid scrub-grassland and Zagros semiarid and humid forest, and between arid desert scrub and arid desert life zones. The Hyrcanian humid forest life zone had no overlap with 4 life zones but it had a very slight overlap with the Zagros semiarid and humid forest life zone. Arid desert life zone had no overlap with 4 life zones, but a fair overlap with arid desert scrub life zone.

DISCUSSION

The distribution of main life zones of Iran was predicted using seven environmental variables based on CCA analysis. CCA enables simultaneous modeling of all life zones [11]. All environmental and response variables are integrated at the same time in CCA. The efficiency of CCA has been proved in modeling species and communities-environment relationships [3, 16, 11]. Cumulative proportions of variance in the life zone data were low. This is because presence-absence data are often noisy [23]. In addition, an ordination axis that explains only a low amount of variance may still be quite informative [8, 11]. The Kappa values tend to be better than one might expect from the low proportion of variance explained, indicating that the spatial context is being relatively well modeled [11]. Of the environmental variables used in CCA, precipitation was the most important factor in distribution and occurrence of the life zones based on its correlation to CCA axis 1 followed by humidity, elevation, evapotranspiration, mean, maximum and minimum temperature. Chakraborty et al., (2013)[4] stated that the changes in temperature and precipitation cause changes on the area cover and distribution of life zones. Precipitation and temperature are affected by elevation and this effect induces a compression of the typical meridional climatic gradients, causing changes in life zones [6]. The Hyrcanian humid forest life zone, the dense forest of Iran, was found to be distributed



Mohammad Mousaei Sanjerehei

in the regions with high precipitation where mean temperature increases with increasing minimum temperature but decreasing maximum temperature. The Hyrcanian humid forest and arid desert life zones were most efficiently differentiated using CCA based on their scores on ordination axes. Furthermore, the predicted distribution of the Hyrcanian humid forest and arid desert life zones was most accurately predicted, as there was a moderate agreement between the distribution of these two life zones and the reference data, while there was a fair agreement on arid desert scrub, semiarid scrub-grassland and Zagros semiarid and humid forest life zones and a slight agreement on humid grassland life zone. This may be because of three reasons. 1) The Hyrcanian humid forests are dense forests of Iran and both the Hyrcanian humid forest and arid desert life zones are continuously distributed and there is almost no gap within each of these life zones. The other life zones are discontinuously and sparsely distributed throughout Iran. Because of discontinuity and island-like form of these life zones, the collected data could not show the exact distribution of the life zones, although the extension of these life zones was efficiently predicted. 2) In this research, the potential distribution of the life zones was predicted. So the distribution of the life zones may be accurately predicted, but the human effects, management strategies and environmental disturbances during successional stages have changed the actual status of the life zones to the current status. This is obvious for the north and northwest parts of Iran where the vast area of humid grasslands and semiarid scrub-grasslands has been changed into agricultural lands and dry farmlands. 3) More detailed data such as soil properties are required for accurately determining the distribution of the life zones. Although CCA could distinguish between the life zones, the overlap between the predicted distribution of humid grassland, Zagros semiarid and humid forest and semiarid scrub-grassland life zones and between arid desert scrub and arid desert life zones indicated that CCA cannot efficiently model and delimit the life zones which have approximately similar environmental conditions. Instead, the accurate predicted distribution of the Hyrcanian humid forest and arid desert life zones and a lack of overlap between these two life zones and the four other life zones showed that CCA enables to efficiently distinguish and delimit the life zones with very humid and very arid climate.

REFERENCES

1. Allen RG, Pereira LS, Raes D, and Smith M. Crop evapotranspiration-Guidelines for computing crop water requirements-FAO Irrigation and drainage paper 56. FAO, Rome, 300, 6541; 1996.
2. Box EO. Predicting physiognomic vegetation types with climate variables. *Vegetatio* 1981; 45(2), 127-139.
3. Chahouki MAZ, Ahvazi LK, and Azarnivand H. Comparison of three modeling approaches for predicting plant species distribution in mountainous scrub vegetation (Semnan Rangelands, Iran). *Polish Journal of Ecology* 2012; 60(2), 277-289.
4. Chakraborty A, Joshi PK, Ghosh A, and Arendran G. Assessing biome boundary shifts under climate change scenarios in India. *Ecological Indicators* 2013; 34, 536-547.
5. Congalton RG, and Green K. Assessing the accuracy of remotely sensed data: principles and practices. CRC press. 2008.
6. Diaz HF, Villalba R, Greenwood G, and Bradley RS. The impact of climate change in the American Cordillera. *Eos, Transactions American Geophysical Union* 2006; 87(32), 315-315.
7. Dubuis A, Giovanettina S, Pellissier L, Pottier J, Vittoz P, and Guisan A. Improving the prediction of plant species distribution and community composition by adding edaphic to topo-climatic variables. *Journal of Vegetation Science* 2013; 24(4), 593-606.
8. Gauch HG. *Multivariate Analysis in Community Ecology*. Cambridge University Press, Cambridge. 1982.
9. Guisan A, Edwards Jr, TC, and Hastie T. Generalized linear and generalized additive models in studies of species distributions: setting the scene. *Ecological modeling* 2002; 157(2), 89-100.
10. Guisan A, and Thuiller W. Predicting species distribution: offering more than simple habitat models. *Ecology letters* 2005; 8(9), 993-1009.
11. Guisan A, Weiss SB, and Weiss AD. GLM versus CCA spatial modeling of plant species distribution. *Plant Ecology* 1999; 143(1), 107-122.
12. Hill MO. Correspondence analysis: a neglected multivariate method. *Appl. Stat.* 23: 340–354. 1974.



Mohammad Mousaei Sanjerehei

13. Holdridge LR. Life zone ecology. (rev. ed.). 1967.
14. Landis JR, and Koch GG. The measurement of observer agreement for categorical data. *Biometrics* 1977; 159-174.
15. Minchin PR. An evaluation of the relative robustness of techniques for ecological ordination. In *Theory and models in vegetation science* (pp. 89-107). Springer Netherlands. 1987.
16. Ohmann JL, and Gregory MJ. Predictive mapping of forest composition and structure with direct gradient analysis and nearest-neighbor imputation in coastal Oregon, USA. *Canadian Journal of Forest Research* 2002; 32(4), 725-741.
17. Scott JM, Heglund PJ, Morrison ML, Haufler JB, Raphael MG, Wall WA, and Samson FB. Predicting species occurrences: issues of scale and accuracy. *Predicting species occurrences: Issues of scale and accuracy*. 2002.
18. Smolik MG, Dullinger S, Essl F, Kleinbauer I, Leitner M, Peterseil J, and Vogl G. Integrating species distribution models and interacting particle systems to predict the spread of an invasive alien plant. *Journal of Biogeography* 2010; 37(3), 411-422.
19. Ter Braak C J, and Looman CW. Weighted averaging, logistic regression and the Gaussian response model. *Vegetatio* 1986; 65(1), 3-11.
20. Ter Braak CJ. Canonical correspondence analysis: a new eigenvector technique for multivariate direct gradient analysis. *Ecology* 1986; 67(5), 1167-1179.
21. Ter Braak CJ. The analysis of vegetation-environment relationships by canonical correspondence analysis. In *Theory and models in vegetation science* (pp. 69-77). Springer Netherlands. 1987.
22. Ter Braak CJ, and Verdonschot PF. Canonical correspondence analysis and related multivariate methods in aquatic ecology. *Aquatic sciences* 1995; 57(3), 255-289.
23. Ter Braak CJF. CANOCO: an extension of DECORANA to analyze species-environment relationships *Vegetatio* 1988; 75: 159– 160.
24. Wohlgenuth T, Nobis MP, Kienast F, and Plattner M. Modelling vascular plant diversity at the landscape scale using systematic samples. *Journal of Biogeography* 2008; 35(7), 1226-1240.
25. Zimmermann NE, and Kienast F. Predictive mapping of alpine grasslands in Switzerland: species versus community approach. *Journal of Vegetation Science* 1999; 10(4), 469-482

Table 1: Characteristics of the four first ordination axes.

Axis	1	2	3	4
Eigenvalues	0.783	0.54	0.216	0.077
Life zone- environment correlations	0.885	0.735	0.465	0.277
% of variance of life zone data	15.7	10.8	4.3	1.5
Cumulative % variance of life zone data	15.7	26.5	30.8	32.3
Cumulative % variance of life zone- environment relation	48	81.1	94.4	99.1

Monte Carlo permutation test showed that all canonical axes were significant ($P = 0.002$).



Mohammad Mousaei Sanjerehei

Table 2 : Canonical (regression) coefficients of variables, correlation of ordination axis with each environmental predictor and t-value of regression coefficient. ETo: reference evapotranspiration, Tmax: maximum temperature, Tmin: minimum temperature, H: relative humidity, E: elevation, P: precipitation and Tmean: mean temperature.

Variable	Canonical coefficients				Correlation coefficients				t-values			
	Ax1	Ax 2	Ax3	Ax4	Ax1	Ax 2	Ax 3	Ax4	Ax1	Ax 2	Ax 3	Ax4
ETo	-0.199	-0.07	0.241	0.501	-0.81	0.24	-0.31	0.11	-2.66	-0.64	1.69	3.24
Tmax	0.417	-0.266	-1.193	-0.104	-0.62	0.40	-0.55	0.17	4.73	-2.07	-7.12	-0.57
Tmin	-0.315	0.173	0.662	0.098	-0.44	0.50	-0.36	0.41	-4.65	1.75	5.13	0.70
H	0.302	-0.329	-0.326	0.523	0.82	0.05	0.13	0.41	5.1	-3.82	-2.9	4.28
E	-0.055	-0.391	-0.370	-0.018	0.18	-0.81	-0.27	-0.19	-1.51	-7.42	-5.38	-0.24
P	0.550	0.527	-0.069	-0.16	0.94	0.17	-0.07	-0.06	15.87	10.43	-1.04	-2.24
Tmean	-0.155	0.518	-0.251	-0.192	-0.58	0.73	-0.25	0.14	-2.92	6.71	-2.49	-1.76

Table 3: Kappa coefficient and related Z- statistic for the predicted distribution of Iran life zones

Life zone	Kappa	Z- statistic	Strength of agreement
Hyrceanian humid forest	0.57	103.1**	Moderate
Arid desert	0.51	260.6**	Moderate
Semiarid scrub-grassland	0.22	108.8**	Fair
Zagros semiarid and humid forest	0.22	103.6**	Fair
Arid desert scrub	0.21	119**	Fair
Humid grassland	0.16	71.2**	Slight

** : significant at 0.01 probability level.

Table 4: kappa value between the predicted distribution of the life zones.

Life zone	Hyrceanian humid forest	Zagros semiarid and humid forest	Humid grassland	Semiarid scrub-grassland	Arid desert scrub	Arid desert
Hurceanian humid forest	-					
Zagros semiarid and humid forest	0.013	-				
Humid grassland	No	0.54	-			
Semiarid scrub-grassland	No	0.23	0.35	-		
Arid desert scrub	No	-0.3	-0.23	-0.02	-	
Arid desert	No	No	No	No	0.2	-

No: There was not any pixel classified as both life zones (no overlap). Kappa =1 indicates maximum overlap between two life zones.



Mohammad Mousaei Sanjerehei

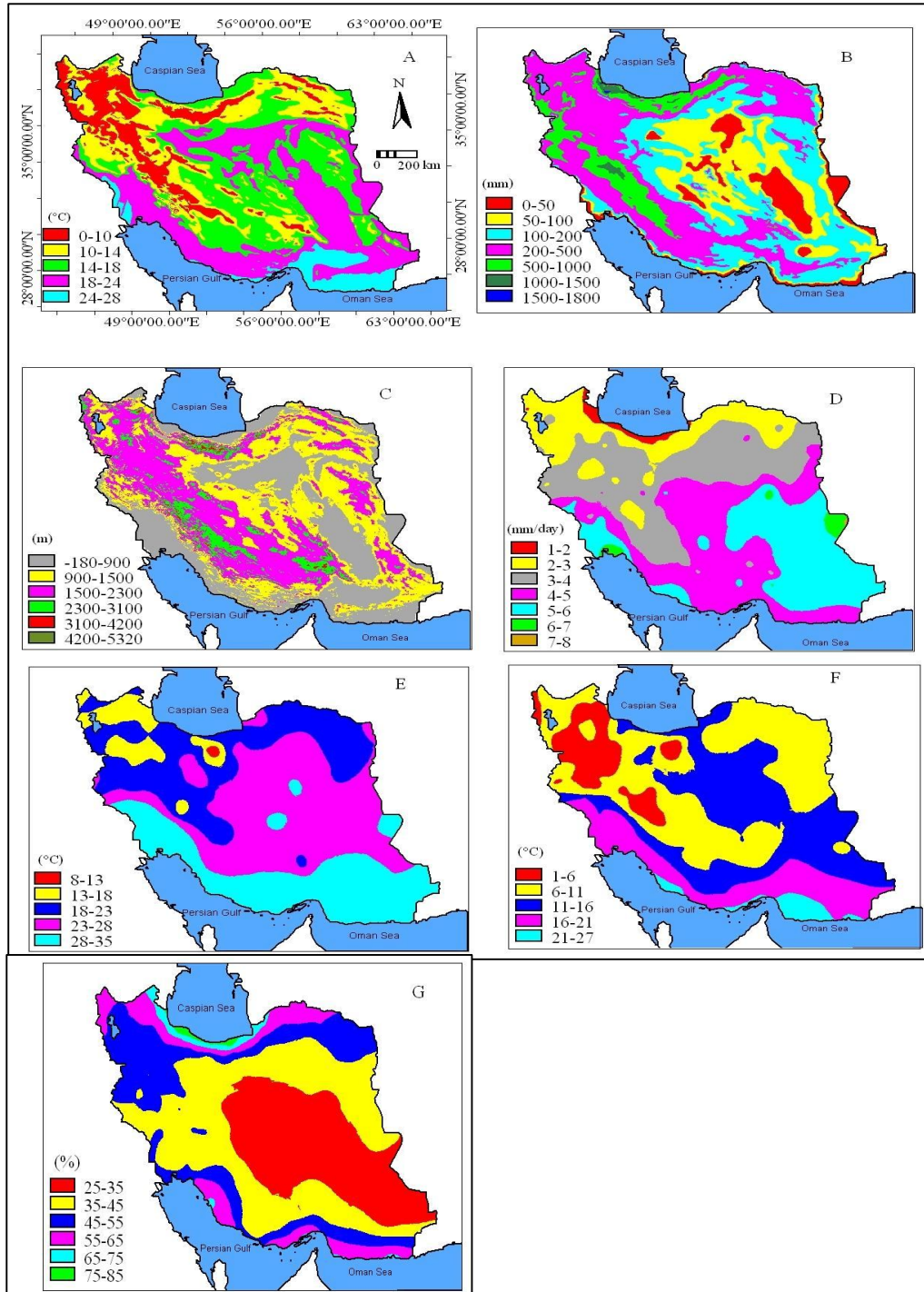


Figure 1- A) Mean annual temperature, B) mean annual precipitation, C) digital elevation model, D) mean annual reference evapotranspiration, E) mean annual maximum temperature, F) mean annual minimum temperature and G) mean annual relative humidity map of Iran based on the data of 1955-2005.



Mohammad Mousaei Sanjerehei

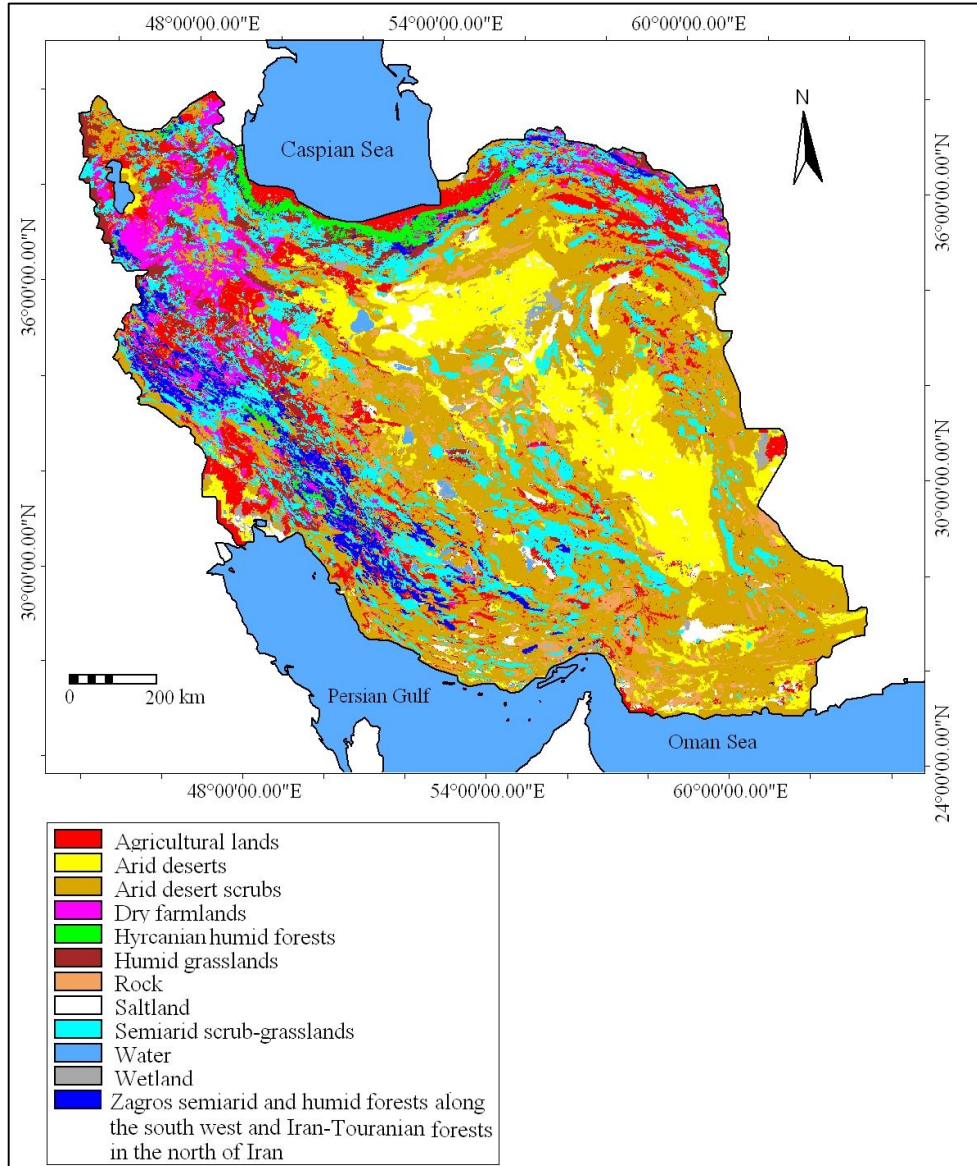


Figure 2- The reference land cover map of Iran in which the life zones including Hyrcanian humid forest, Zagros semiarid and humid forest, humid grassland, semiarid scrub-grassland (semiarid shrub-grassland), arid desert scrub (arid desert shrub) and arid desert life zones are shown together with the other land covers (agricultural lands, dry farmlands, water, saltlands, wetlands and rock).



Mohammad Mousaei Sanjerehei

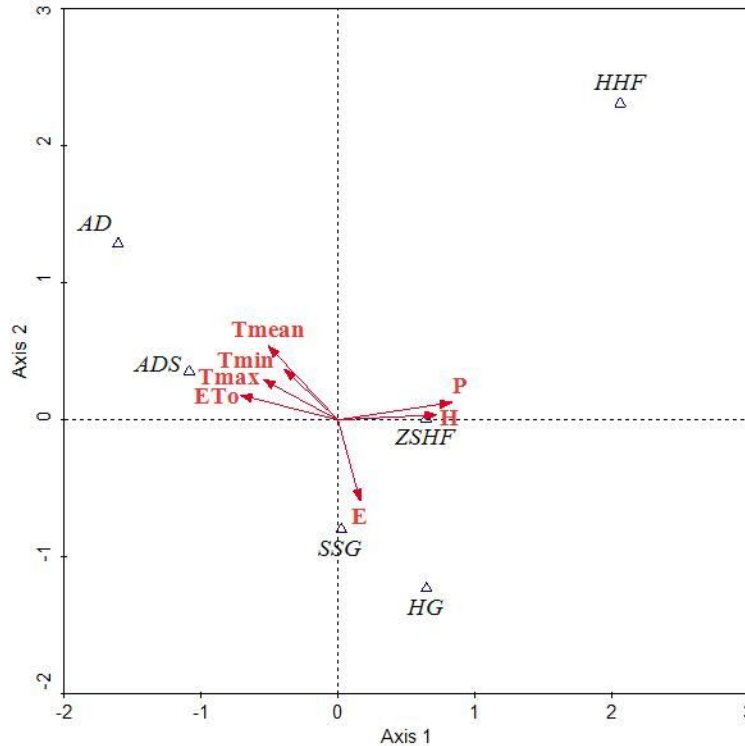


Figure 3- CCA biplots of Iran life zones based on axis 1 versus axis 2. Life zone scores are linear combination scores. ETo: reference evapotranspiration, Tmax: maximum temperature, Tmin: minimum temperature, H: relative humidity, P: precipitation and Tmean: mean temperature, E: elevation. HHF: Hyrcanian humid forest, ZSHF: Zagros semiarid and humid forest, HG: humid grassland, SSG: semiarid scrub-grassland, ADS: arid desert scrub and AD: arid desert life zone.

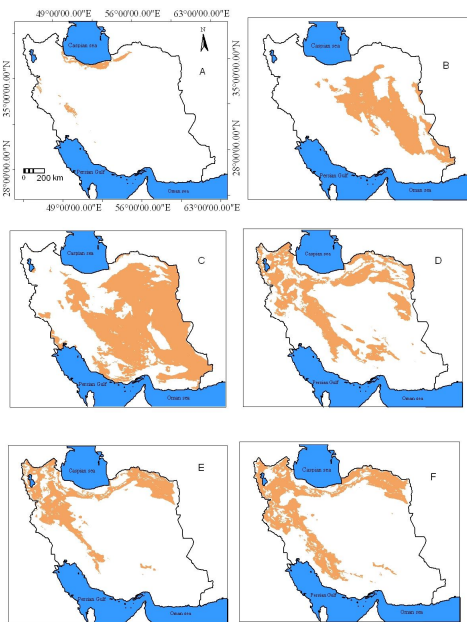


Figure 4 – Potential distribution map of A) Hyrcanian humid forest, B) Arid desert, C) Arid desert scrub, D) Semiarid scrub-grassland, E) Humid grassland and F) Zagros semiarid and humid forest life zones modeled by CCA. Predictive distribution range of each life zone is based on one standard deviation unit distance from the centroid of the life zone observation.



New Radial Velocity Studies and Curve Analysis of RX J0529.3+1210, WW Cam, ω Dra and HD 197770.

Ghaderi K*, Gh. Nikraftar, M. H. Baghadam , A. Rahmani and S. Ghasema.

Department of Science and Engineering, Islamic Azad University, Marivan Branch, Marivan, Iran.

Received: 12 May 2014

Revised: 28 May 2014

Accepted: 28 May 2014

*Address for correspondence

Ghaderi K,
Department of Science and Engineering,
Islamic Azad University,
Marivan Branch,
Marivan, Iran.
E.mail: k.ghaderi.60@gmail.com.



This is an Open Access Journal / article distributed under the terms of the **Creative Commons Attribution License** (CC BY-NC-ND 3.0) which permits unrestricted use, distribution, and reproduction in any medium, provided the original work is properly cited. All rights reserved.

ABSTRACT

Using measured radial velocity data of four double-lined spectroscopic binary systems RX J0529.3+1210, WW Cam, ω Dra and HD 197770, we find corresponding orbital and spectroscopic elements via a Probabilistic Neural Network (PNN). Our numerical results are in good agreement with those obtained by others using more traditional methods.

Keywords: spectroscopic binary systems, Probabilistic Neural Network, radial velocity data.

INTRODUCTION

Analysis of both light and radial velocity (hereafter V_R) curves of binary systems helps us to determine the masses and radii of individual stars. One historically well-known method to analyze the V_R curve is that of Lehmann-Filhés [1]. Some other methods were also introduced by Sterne [2] and Petrie [3]. The different methods of the V_R curve analysis have been reviewed in ample detail by Karami & Teimoorinia [4]. Karami & Teimoorinia [4] also proposed a new non-linear least squares velocity curve analysis technique for spectroscopic binary stars. They showed the validity of their new method to a wide range of different types of binary See Karami & Mohebi [5-7] and Karami et al. [8]. Artificial Neural Networks have become a popular tool in almost every field of science. In recent years, ANNs have been widely used in astronomy for applications such as star/galaxy discrimination, morphological classification of galaxies, and spectral classification of stars (see Bazarghan et al. [9] and references therein). Following Bazarghan et al. [9], we employ Probabilistic Neural Networks (PNNs). This network has been investigated in ample details by Bazarghan et al. [9]. Probabilistic Neural Network (PNN) is a new tool to derive the orbital parameters of the spectroscopic binary stars.



Ghaderi et al.

In the present paper we use a Probabilistic Neural Network (PNN) to find the optimum match to the four parameters of the V_R curves of the four double-lined spectroscopic binary systems: RX J0529.3+1210, WW Cam, ω Dra and HD 197770. Our aim is to show the validity of our new method to a wide range of different types of binary. RX J0529.3+1210 is the most eccentric pre-main sequence double-lined binary known to date and this system is a member of the 32 Ori moving group. The spectral type of this system is K7-M0 and the orbital period is $P=461.89$ days [10]. WW Cam is a double-lined eclipsing binary star and the components of WW Cam are main-sequence stars with an age of about 490 Myr. The spectral type is A4m and the orbital period is $P=2.27436322$ days [11]. ω Dra is a double-lined spectroscopic binary and consists of primary and secondary components. The spectral type is F5V and the orbital period is $P=5.2798088$ days [12]. HD 197770 is an eclipsing double-lined spectroscopic binary and both components of HD 197770 have spectral types near B2 III and the orbital period of the system is $P=99.6918$ days [13].

This paper is organized as follows. In Sect. 2, we introduce a Probabilistic Neural Network (PNN) to estimate the four parameters of the V_R curve. In Sect. 3, the numerical results are reported, while the conclusions are given in Sect. 4.

V_R curve parameters estimation by the Probabilistic Neural Network (PNN)

Following Smart [14], the V_R of a star in a binary system is defined as follows

$$V_R = \gamma + K[\cos(\theta + \omega) + e \cos \omega] \quad (1)$$

where γ is the V_R of the center of mass of system with respect to the sun. Also K is the amplitude of the V_R of the star with respect to the center of mass of the binary. Furthermore θ, ω and e are the angular polar coordinate (true anomaly), the longitude of periastron and the eccentricity, respectively. Here we apply the PNN method to estimate the four orbital parameters, γ, K, e and ω of the V_R curve in Eq. (1). In this work, for the identification of the observational V_R curves, the input vector is the fitted V_R curve of a star. The PNN is first trained to classify V_R curves corresponding to all the possible combinations of γ, K, e and ω . For this one can synthetically generate V_R curves given by Eq. (1) for each combination of the parameters:

- $-100 \leq \gamma \leq 100$ in steps of 1;
- $1 \leq K \leq 300$ in steps of 1;
- $0 \leq e \leq 1$ in steps of 0.001;
- $0 \leq \omega \leq 360^\circ$ in steps of 5;

This gives a very big set of k pattern groups, where k denotes the number of different V_R classes, one class for each combination of γ, K, e and ω . Since this very big number of different V_R classes leads to some computational limitations, hence one can first start with the big step sizes. Note that from Petrie [3], one can guess γ, K and e from a V_R curve. This enable one to limit the range of parameters around their initial guesses. When the preliminary orbit was derived after several stages, then one can use the above small step sizes to obtain the final orbit. The PNN has four layers including input, pattern, summation, and output layers, respectively (see Fig. 5 in Bazarghan et al. [9]). When an input vector is presented, the pattern layer computes distances from the input vector to the training input vectors and produces a vector whose elements indicate how close the input is to a training input. The summation layer sums these contributions for each class of inputs to produce as its net output a vector of probabilities. Finally, a competitive transfer function on the output layer picks the maximum of these probabilities, and produces a 1 for that class and a 0 for the other classes [15,16]. Thus, the PNN classifies the input vector into a specific k class labeled by the four parameters γ, K, e and ω because that class has the maximum probability of being correct.



Ghaderi et al.

Numerical Results

Here, we use the PNN to derive the orbital elements for the four different double-lined spectroscopic systems RX J0529.3+1210, WW Cam, ω Dra and HD 197770. Using measured V_R data of the two components of these systems obtained by Mace et al. [10] for RX J0529.3+1210, Sandberg Lacy et al. [11] for WW Cam, Behr et al. [12] for ω Dra and Gordon et al. [13] for HD 197770, the fitted velocity curves are plotted in terms of the phase in Figs. 1 to 4.

The orbital parameters obtaining from the PNN for RX J0529.3+1210, WW Cam, ω Dra and HD 197770 are tabulated in Tables 1, 3, 5 and 7, respectively. Tables show that the results are in good accordance with the those obtained by Mace et al. [10] for RX J0529.3+1210, Sandberg Lacy et al. [11] for WW Cam, Behr et al. [12] for ω Dra and Gordon et al. [13] for HD 197770.

Note that the Gaussian errors of the orbital parameters in Tables 1, 3, 5 and 7 are the same selected steps for generating V_R curves, i.e. $\Delta\gamma = 1, \Delta K = 1, \Delta e = 0.001$ and $\Delta\omega = 5$. These are close to the observational errors reported in the literature. Regarding the estimated errors, following Specht [16], the error of the decision boundaries depends on the accuracy with which the underlying Probability Density Functions (PDFs) are estimated. Parzen [17] proved that the expected error gets smaller as the estimate is based on a large data set. This definition of consistency is particularly important since it means that the true distribution will be approached in a smooth manner. Specht [16] showed that a very large value of the smoothing parameter would cause the estimated errors to be Gaussian regardless of the true underlying distribution and the misclassification rate is stable and does not change dramatically with small changes in the smoothing parameter. The combined spectroscopic elements including $m_p \sin^3 i$, $m_s \sin^3 i$, $(m_p + m_s) \sin^3 i$, $(a_p + a_s) \sin i$ and $\frac{m_s}{m_p}$ are calculated by substituting the estimated parameters

K, e and ω in to Eqs. (3), (15) and (16) in Karami and Teimoorinia [4]. The results obtained for the four systems are tabulated in Tables 2, 4, 6 and 8 show that our results are in good agreement with the those obtained by Mace et al. [10] for RX J0529.3+1210, Sandberg Lacy et al. [11] for WW Cam, Behr et al. [12] for ω Dra and Gordon et al. [13] for HD 197770, respectively. Here the errors of the combined spectroscopic elements in Tables 2, 4, 6 and 8 are obtained by the help of orbital parameters errors. See again Eqs. (3), (15) and (16) in Karami and Teimoorinia [4].

The results obtained for the four systems are tabulated in Tables 2, 4, 6 and 8 show that our results are in good agreement with the those obtained by Mace et al. [10] for RX J0529.3+1210, Sandberg Lacy et al. [11] for WW Cam, Behr et al. [12] for ω Dra and Gordon et al. [13] for HD 197770, respectively. Here the errors of the combined spectroscopic elements in Tables 2, 4, 6 and 8 are obtained by the help of orbital parameters errors. See again Eqs. (3), (15) and (16) in Karami and Teimoorinia [4].

CONCLUSION

A Probabilistic Neural Network to derive the orbital elements of spectroscopic binary stars was applied. PNNs are used in both regression (including parameter estimation) and classification problems. However, one can discretize a continuous regression problem to such a degree that it can be represented as a classification problem [15,16], as we did in this work. Using the measured V_R data of RX J0529.3+1210, WW Cam, ω Dra and HD 197770 obtained by Mace et al. [10], Sandberg Lacy et al. [11], Behr et al. [12] and Gordon et al. [13], respectively, we find the orbital elements of these systems by the PNN. Our numerical results shows that the results obtained for the orbital and spectroscopic parameters are in good agreement with those obtained by others using more traditional methods.



Ghaderi et al.

This method is applicable to orbits of all eccentricities and inclination angles. In this method the time consumed is considerably less than the method of Lehmann-Filhés. It is also more accurate as the orbital elements are deduced from all points of the velocity curve instead of four in the method of Lehmann-Filhés. The present method enables one to vary all of the unknown parameters γ , K , e and ω simultaneously instead of one or two of them at a time. It is possible to make adjustments in the elements before the final result is obtained. There are some cases, for which the geometrical methods are inapplicable, and in these cases the present one may be found useful. One such case would occur when observations are incomplete because certain phases could have not been observed. Another case in which this method is useful is that of a star attended by two dark companions with commensurable periods. In this case the resultant velocity curve may have several unequal maxima and the geometrical methods fail altogether.

REFERENCES

1. R. Lehmann-Filhés, AN. 136, 17 (1984).
2. T. E. Sterne, PNAS. 27, 175 (1941).
3. R. M. Petrie, "Astronomical Techniques," Ed., W. A. Hiltner, University of Chicago Press, Chicago (1960).
4. K. Karami and H. Teimoorinia, Ap&SS. 311, 435 (2007).
5. K. Karami and R. Mohebi, ChJAA. 7, 668 (2007).
6. K. Karami and R. Mohebi, JApA. 28, 217 (2007).
7. K. Karami and R. Mohebi, JApA. 30, 153 (2009).
8. K. Karami, R. Mohebi and M. M. Soltanzadeh, Ap&SS. 318, 69 (2008).
9. M. Bazarghan, H. Safari, D. E. Innes, E. Karami and S. K. Solanki, A&A, 492, L13 (2008).
10. G. N. Mace, L. Prato, L. H. Wasserman, G. H. Schaefer, O. G. Franz and M. Simon, AJ. 137, 3478 (2009).
11. C. H. Sandberg Lacy, G. Torres, A. Claret and J. A. Sabby, AJ. 123, 1013 (2002).
12. B. B. Behr, A. T. Cenko, A. R. Hajian, R. S. McMillan, M. Murison, J. Meade and R. Hindsley, AJ. 142, 6B (2011).
13. K. D. Gordon, G. C. Clayton, T. L. Smith, J. P. Aufdenberg, J. S. Drilling, M. M. Hanson, C.M. Anderson and C. L. Mulliss, AJ. 115, 2561 (1998).
14. W. M. Smart, "Textbook on Spherical Astronomy," Sixth Ed., Revised by R. M. Green, Cambridge Univ. Press, 360 (1990).
15. D. F. Specht, "in Proc IEEE International Conference on Neural Networks," 525 (1988).
16. D. F. Specht, Neural Networks, 3, 109 (1990).
17. E. Parzen, Annals of Mathematical Statistics, 33, 1065 (1962).

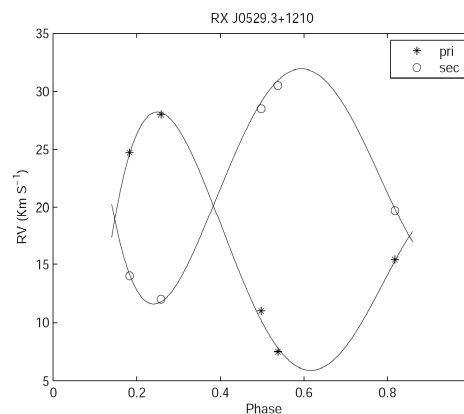


Fig. 1: Radial velocities of the primary and secondary components of RX J0529.3+1210 plotted against the phase. The observational data have been measured by Mace et al. [10].



Ghaderi et al.

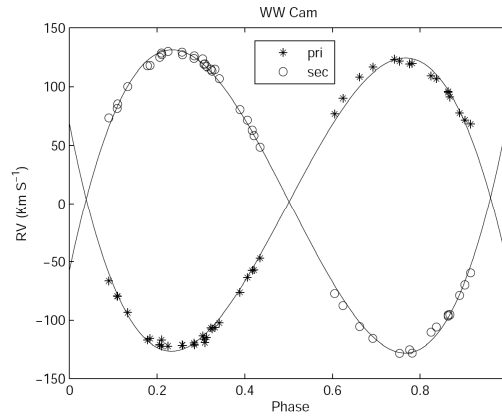


Fig. 2: Radial velocities of the primary and secondary components of WW Cam plotted against the phase. The observational data have been measured by Sandberg Lacy et al. [11].

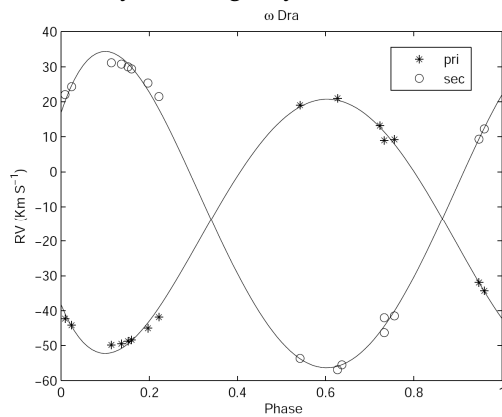


Fig. 3: Radial velocities of the primary and secondary components of ω Dra plotted against the phase. The observational data have been measured by Behr et al. [12].

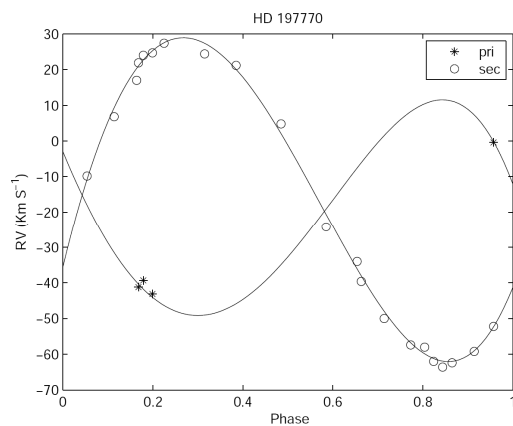


Fig. 4: Radial velocities of the primary and secondary components of HD 197770 plotted against the phase. The observational data have been measured by Gordon et al. [13].



Ghaderi et al.

Table 1: Orbital parameters of RX J0529.3+1210

	This Paper	Mace et al. [10]
$\gamma (kms^{-1})$	18 ± 1	18.38 ± 0.30
$K_p (kms^{-1})$	23 ± 1	22.76 ± 1.59
$K_s (kms^{-1})$	31 ± 1	31.25 ± 9.44
e	0.879 ± 0.001	0.88 ± 0.02
$\omega(^{\circ})$	105 ± 5	108 ± 4

Table 2: Combined spectroscopic elements of RX J0529.3+1210

Parameter	This Paper	Mace et al. [10]
$m_p \sin^3 i / M_{\odot}$	0.4690 ± 0.0553	0.454 ± 0.312
$m_s \sin^3 i / M_{\odot}$	0.3479 ± 0.0449	0.330 ± 0.317
$(m_p + m_s) \sin^3 i / M_{\odot}$	0.8169 ± 0.1002	—
$a_p \sin i / 10^6 km$	67.6556 ± 3.2978	67.98 ± 2.05
$a_s \sin i / 10^6 km$	93.8837 ± 3.3915	93.32 ± 27.57
$(a_p + a_s) \sin i / 10^6 km$	163.5394 ± 6.6893	—
m_s / m_p	0.7419 ± 0.0619	0.73 ± 0.23

Table 3: Orbital parameters of WW Cam

	This Paper	Sandberg Lacy et al. [11]
$\gamma (kms^{-1})$	1 ± 1	0.91 ± 0.30
$K_p (kms^{-1})$	125 ± 1	124.62 ± 0.58
$K_s (kms^{-1})$	128 ± 1	127.76 ± 0.31
e	0.008 ± 0.001	0.0094 ± 0.0015
$\omega(^{\circ})$	130 ± 5	134 ± 10

Table 4: Combined spectroscopic elements of WW Cam

Parameter	This Paper	Sandberg Lacy et al. [11]
$m_p \sin^3 i / M_{\odot}$	1.9304 ± 0.0456	1.917 ± 0.013
$m_s \sin^3 i / M_{\odot}$	1.8852 ± 0.0449	1.870 ± 0.018
$(m_p + m_s) \sin^3 i / M_{\odot}$	3.8156 ± 0.0906	—
$a_p \sin i / 10^6 km$	3.9092 ± 0.0313	3.897 ± 0.019
$a_s \sin i / 10^6 km$	4.0030 ± 0.0313	3.995 ± 0.010
$(a_p + a_s) \sin i / R_{\odot}$	11.3682 ± 0.0900	11.340 ± 0.030
m_s / m_p	0.9766 ± 0.0155	0.9755 ± 0.0053

Table 5: Orbital parameters of ω Dra

	This Paper	Behr et al. [12]
$\gamma (kms^{-1})$	-13 ± 1	-13.501 ± 0.016
$K_p (kms^{-1})$	36 ± 1	36.292 ± 0.020
$K_s (kms^{-1})$	45 ± 1	44.718 ± 0.038
e	0.002 ± 0.001	0.0023 ± 0.0006
$\omega(^{\circ})$	135 ± 5	137.86 ± 13.48

Table 6: Combined spectroscopic elements of ω Dra

Parameter	This Paper	Behr et al. [12]
$m_p \sin^3 i / M_{\odot}$	0.1615 ± 0.0116	0.16054 ± 0.00030
$m_s \sin^3 i / M_{\odot}$	0.1292 ± 0.0100	0.13029 ± 0.00018
$(m_p + m_s) \sin^3 i / M_{\odot}$	0.2907 ± 0.0215	—
$a_p \sin i / R_{\odot}$	3.7553 ± 0.1043	—
$a_s \sin i / R_{\odot}$	4.6941 ± 0.1043	—
$(a_p + a_s) \sin i / R_{\odot}$	8.4494 ± 0.2086	—
m_s / m_p	0.8000 ± 0.0400	—

Table 7: Orbital parameters of HD197770

	This Paper	Gordon et al. [13]
$\gamma (kms^{-1})$	-15 ± 1	-15.31 ± 0.32
$K_p (kms^{-1})$	31 ± 1	31.21 ± 0.81
$K_s (kms^{-1})$	47 ± 1	47.05 ± 0.36
e	0.146 ± 0.001	0.147 ± 0.008
$\omega(^{\circ})$	65 ± 5	69.76 ± 3.34

Table 8: Combined spectroscopic elements of HD 197770

Parameter	This Paper	Gordon et al. [13]
$m_p \sin^3 i / M_{\odot}$	2.8595 ± 0.2088	2.89 ± 0.08
$m_s \sin^3 i / M_{\odot}$	1.8861 ± 0.1584	1.92 ± 0.09
$(m_p + m_s) \sin^3 i / M_{\odot}$	4.7456 ± 0.3672	—
$a_p \sin i / R_{\odot}$	60.4042 ± 1.9575	60.8 ± 1.6
$a_s \sin i / R_{\odot}$	91.5805 ± 1.9622	91.7 ± 0.7
$(a_p + a_s) \sin i / R_{\odot}$	151.9847 ± 3.9197	—
m_s / m_p	0.6596 ± 0.0355	—



Antimicrobial Activity of *Colocasia esculenta* (L.)Schott Stem Extract and Use as a Natural Indicator in Acid Base Titration.

Kamlesh Niranjane*, Smita Mujbaile, Bhushan Pahune, Dipnesh Bhaskarwar and Sandhya Bagde.

Department of Pharmaceutical chemistry, Dadasaheb Balpande College of Pharmacy, Besa, Nagpur-440034 (M.S.) India.

Received: 24 April 2014

Revised: 20 May 2014

Accepted: 28 May 2014

*Address for correspondence

Kamlesh Niranjane,
Assistant Professor, Department of Pharmaceutical Chemistry,
Dadasaheb Balpande College of Pharmacy,
Besa, Nagpur-440034 (M.S.) India.
E.mail: kamleshniranjane24@rediffmail.com



This is an Open Access Journal / article distributed under the terms of the **Creative Commons Attribution License** (CC BY-NC-ND 3.0) which permits unrestricted use, distribution, and reproduction in any medium, provided the original work is properly cited. All rights reserved.

ABSTRACT

Now a day natural indicators are more widely prepared as it has several advantages over synthetic one. Mostly flowers and fruits extracts are used for the preparation of natural indicators. In this research work stem part of *Colocasia esculenta* used as natural indicator. *Colocasia esculenta* is a species of the *Colocasia* genus, belonging to the family Araceae. The present work highlights the use of *Colocasia esculenta* stem extract as an acid base indicator in different types of acid base titrations. The equivalence points obtained by the stem extract coincident with the equivalence points obtained by standard indicators. In case of weak acid and weak base titration, the results obtained by the stem extract matched with the results obtained by mixed indicator and also the prepared stem extract were tested for antimicrobial activity against *staphylococcus aureus* and showed significant antimicrobial activity. This natural indicator was found to be very useful, economical, simple and accurate for the said titration.

Key Words: *Colocasia esculenta*, Acid base indicator, Natural indicator, Antimicrobial activity.

INTRODUCTION

Plants have played an important role in maintaining human health. Apart from this it shows a wide property for the preparation of many chemicals. In present Scenario natural indicator are mostly prepared over synthetic one. *Colocasia esculenta* commonly known as Taro, Alu (Marathi), Arbi (Hindi) and Colocasia (English) is a species of the *Colocasia* genus, belonging to the family Araceae [1]. It is native to tropical Asia and Polynesia [2] and considered an evergreen perennial tuberous herb. *Colocasia* has given us lots of pleasure all summer along with its huge, velvet-like

**Kamlesh Niranjane et al.**

textured, dark green, heart-shaped leaves that are lined with darker veins, adding real drama to the shade garden near our pond. These are herbaceous perennial herb plants with large corms on or just below the ground surface. The leaves are large to very large, 20–150 cm (7.9–59 in) long, with a sagittate shape. Due to its shape of leaves like a large ear or shield, it commonly called as elephant's-ear plant. The plant reproduces mostly by means of rhizomes (tubers, corms) but it also produces "clusters of two to five fragrant inflorescences in the leaf axils" [3]. It's also spectacular as a sturdy backdrop for perennials in the flower border, although we suspect in most full sun situations, it will perform better if a soaker hose provides a little constant moisture. Excellent for water gardens when planted in a pot submerged in the pond. Bulb sizes differ depending on variety of plant 18" on center; zones 8-11. The leaf juice of the plant is styptic, stimulant and rubefacient, and is useful in internal hemorrhages, otalgia, adenitis and buboes. The juice of the corm is laxative, demulcent and anodyne [4]. The plant also shows antidibatic activity [5], antimicrobial activity [6], anti-helminthiasis activity [7] and anti-inflammatory activity [8]. The plant contains wide number of anthocyanin present in almost all part of herb. After phytochemical investigations on the *Colocasia* extracts it proven to be presence of anthocyanins such as cyanidin-3-glucoside, pelargonidin-3-glucoside and cyanidin-3-rhamnoside, which have antioxidant activities as evident from previous studies [9, 10, 11].

MATERIALS AND METHODS**Plant profile**

Colocasia esculenta Linn. (Family: Araceae) is also known as *Arum esculentum* L. and *Colocasia antiquorum* Schott. [12] It is commonly called as *taro* (English); *alavi*, *patarveli* (Gujarati); *arvi*, *kachalu* (Hindi); *alu* (Marathi); *alupam*, *alukam* (Sanskrit); and *sempu* (Tamil). Geographically, it occurs throughout India and is cultivated worldwide.[13, 14]

All the apparatus and instruments required for the present research work were calibrated [15, 16]. Analytical grade reagents were made available by Dadasaheb Balpande college of Pharmacy, Besa Nagpur. Reagents and volumetric solutions were prepared as per standard books [17, 18]. The stems of *Colocasia esculenta* plant were collected from the Nagpur region in the month of November 2013. The plant was identified and authenticated at Department of Botany, R.T.M. Nagpur University, Nagpur.

Solvent Extraction

The fresh stems were cut into small pieces and kept at room temperature. The small pieces of stems were dried, ground into fine powder with a mechanical blender. The resulting powder was extracted with water. From these solutions, anthocyanins were isolated by using ether [19]. Finally extract was filtered and used as indicator in several acid base titrations. The experimental work was carried out by using the same set of glasswares for all type of titrations. As the same aliquots were used for both titrations i.e. titration by using standard indicator and stems extract. The equimolar titrations were performed using 25 ml of titrant with three drops of indicator. All the parameters for experiment are given in Table 1. A set of five experiments was carried out. The mean and standard deviation were calculated from results and also the solvent extracts were concentrated under reduced pressure and preserved at 5°C in airtight bottle until further use for antimicrobial activity.

Stock Solution

Prepared stem extract (50 mg) were dissolved in DMF (10ml) and volume was made up to 100 ml to produce a concentration of 500 µg/ml. Further dilutions were made with DMF to produce 50, 100, 200 µg/ml.



Kamlesh Niranjane et al.

Procedure for antimicrobial activity [20]

All the operations were carried out under aseptic conditions. Sterile medium was melted on water bath and kept at 45°C in constant temperature water bath. In each sterile petri dish molten medium was added so that thickness was approximately 4-5 mm and sub cultured organism under study was inoculated. The inoculated dishes were allowed to set for 30 min. at room temperature. Cups of 6 mm diameter were then made with the help of sterile stainless still bore; 1 ml of test solution of stem extract was added to each cup. Petri dishes were kept in refrigerator for 30 minutes so as to allow diffusion of the solution in the medium, and then incubated at 37°C for 24 hrs. for antibacterial activity. Zone of inhibition produced by test compounds were measured in mm and the compounds were selected on the basis of their MIC. The results are shown in Table 3.

RESULTS AND DISCUSSION

The Prepared stem extract was screened for its use as an acid base indicator in various acid base titrations, and result of screening compared with the result obtained by standard indicators methyl red , phenolphthalein and mixed indicator methyl orange: bromocresol green (0.1:0.2)] for strong acid v/s strong base (HCl and NaOH), strong acid v/s weak base (HCl and NH₄OH), weak acid v/s weak base (oxalic acid and NH₄OH) titrations respectively[21,22]. All these parameters are shown in Table 1. For all titrations the equivalence points obtained by the stem extract matched with the equivalence points obtained by standard indicators. The results of screening were listed in Table 2. The prepared stem extract were also screened for antimicrobial activity against *S. aureus* using agar diffusion method and the result obtained are shown in Table 3.

CONCLUSION

It is concluded from the data, the antimicrobial activity is directly proportional to concentration. As increase in concentration of solution results in an increase in zone of inhibition, and also the present research work of the *Colocasia esculenta* stem extract alone can serve the purpose of indicator in weak acid and weak base titration, where generally mixed indicators employed. Another benefit of this titration is that it gives colored end point at the equivalence point. The results obtained in all types of acid base titrations lead us to conclude that it was due to the presence of flavonoids and anthocyanins sharp color changes occurred at the end point of the titrations. At last we can say that it is always beneficial to use *Colocasia esculenta* stem extract as an indicator in all types of acid base titrations because of its cost effectiveness, simplicity and availability. This stem extract also have significant antimicrobial activity.

ACKNOWLEDGEMENTS

The authors are very much thankful to Mr. Manoj V. Balpande President and Dr. U.N. Mahajan Principal of Dadasaheb Balpande college of Pharmacy, Besa Nagpur for providing the necessary facilities to carry out the research work. The authors are also grateful to Department of Botany, R.T.M. Nagpur University, Nagpur.

REFERENCES

1. http://en.wikipedia.org/wiki/Colocasia_esculenta, Accessed-15 March 2014.
2. Wagner WL, Herbst DR, and Sohmer SH. Manual of the Flowering Plants of Hawai'i. University of Hawai'i Press/Bishop Museum Press. 1999; 2: 1357.
3. Brown, Deni, Aroids. Plants of the Arum Family. Timber Press, Oregon. 2006; 250.
4. "Indian Medicinal Plants", A Compendium of 500 species. Volume-2, Orient Longman, 2003, pp. 160.



Kamlesh Niranjane et al.

5. Kumawat NS, Chaudhari SP, Wani NS, Deshmukh TA, Patil VR. Antidiabetic activity of ethanol extract of *Colocasia esculenta* leaves in alloxan induced diabetic rats International Journal of PharmTech Research 2010; 2(2):1246-1249
6. Singh B, Namrata ,Kumar L, Dwivedi SC. Antibacterial and Antifungal Activity of *Colocasia esculenta* Aqueous Extract: An Edible Plant Journal of Pharmacy Research 2011;4(5):1459-1460
7. Waller PJ 1997. *Veterinary Parasitology* 71, 195–207.
8. Shah BN, Nayak BS, Bhatt SP, Jalalpore SS, Sheth AK. The anti-inflammatory activity of the leaves of *Calocasia esculenta*. *Sau Pharm J* , 2007; 15:3-4
9. Noda y, Kaneyuki T, Mori A, Packer I. Antioxidant activities of pomegranate fruitextract and its anthocyanidins: Delphinidin,cyanidin, and pelargonidin, *Journal of AgriculturalFood Chemistry*, 2002; 50: 166–171
10. Cambie RC, Ferguson LR. Potential functional foods in the traditional Maori diet, *Mutation Research, Fundamental and Molecular Mechanisms of Mutagenesis*, 2003;523–524: 109–117.
11. Kowalczyk E, Kopff A., Fijalkowski P, Niedworok J, Blaszczyk J, Kedziora J. Effects of anthocyanins on selected biochemical parameters in rats exposed to cadmium, *Acta Biochimica Polonica*, 2003;50: 543–548
12. Wiersema JH, Leon B. *World Economic Plants, A standard reference*. New York: CRC Press; 1999. pp. 143.
13. Sheth AK. *The Herbs of Ayurveda*. Ahmedabad: A.K. Sheth Publishers; 2005. pp. 356.
14. Pullaiah T. *Encyclopedia of World Medicinal Plants*. New Delhi: Regency Publication; 2006; 6:18.
15. Jain A. "Practical in modern Pharmaceutical instrumental Analysis", 1st ed., Nirali Prakashan: 2011, p.p.2.5-2.6, 2.16-2.17.
16. Mendham J, Denney RC, Barnes JD, Thomas MJK. "Vogels Textbook of quantitative Analysis", 6th ed., 2000, pp. 69-71.
17. Jeffery GH, Bassett J, Denny RC, Mendham J, "Vogel's Textbook of quantitative chemical analysis" 5th ed., ELBS, Longman groups England: 1996, pp.262.
18. "Anonymous. *The Indian Pharmacopoeia*" 4th ed.,controller of publication, Delhi , 1996 (2),A-208.
19. Agrawal OP. "Chemistry of organic Natural Products". 33rd ed., Krishna Prakashan Media, Meerut (UP):2008 ;(2): pp.166.
20. *Indian Pharmacopoeia* Government of India,Ministry of Health and family welfare,6th ed. published by Indian Pharmacopoeia Commission Ghaziabad:2010;(1):PP.49-56.
21. http://en.Wikipedia.org/wiki/PH_indicator. Accessed – December 10, 2007.
22. Kasture AV, Mahadik KR, Wadodkar SG, More HN. *Pharmaceutical Analysis*,Nirali Prakashan, Pune:2007;(1):pp.6.11-6.12.

Table 1: Analyzed parameters and the comparison of color change.

Titrant	Titrant	Indicator Color Change	
		Standard (p ^H range)	Stem Extract (p ^H range)
HCl	NaOH	Red to Yellow (3.2-11.67)	Pink to Faint yellow(2.8-10.45)
HCl	NH ₄ OH	Colorless to Pink (3.2-8.2)	Pink to Faint yellow (2.8-11.10)
Oxalic acid	NaOH	Red to Yellow (4.7-9.2)	Pink to Faint yellow (1.96-10.26)
Oxalic acid	NH ₄ OH	Orange to Blue-green (4.7-7.8)	Pink to Faint yellow (1.96-11.56)

HCl:- Hydrochloric acid, NaOH:-Sodium Hydroxide , NH₄OH:-Ammonium Hydroxide



Kamlesh Niranjane et al.

Table 2: Screening results of various titrations.

Sr. No.	Titration (Titrant v/s Titrant)	Strength (Moles)	Indicator	Readings with S.D. (+/-)
1	NaOH V/S HCl	0.1	Methyl red	18.4±0.16
			Stem extract	18.5±0.17
		0.5	Methyl red	18.7±0.19
			Stem extract	18.5±0.14
		1	Methyl red	18.7±0.20
			Stem extract	18.9±0.22
2	NH ₄ OH V/S HCl	0.1	Phenolphthalein	12.4±0.13
			Stem extract	12.7±0.17
		0.5	Phenolphthalein	12.8±0.19
			Stem extract	12.6±0.14
		1	Phenolphthalein	12.9±0.20
			Stem extract	12.9±0.21
3	NaOH V/S Oxalic Acid	0.1	Methyl red	21.01±0.22
			Stem extract	21.7±0.26
		0.5	Methyl red	21.8±0.29
			Stem extract	21.9±0.31
		1	Methyl red	21.4±0.28
			Stem extract	21.3±0.26
4	NH ₄ OH V/S Oxalic Acid	0.1	Mixed indicator	10.8±0.23
			Stem extract	10.6±0.15
		0.5	Mixed indicator	10.4±0.16
			Stem extract	10.8±0.18
		1	Mixed indicator	10.5±0.16
			Stem extract	10.5±0.11

HCl: Hydrochloric acid, NaOH: Sodium hydroxide, NH₄OH: Ammonium hydroxide, DMF: Dimethyl Formamide.

Table 3: Antimicrobial activity data against *Staphylococcus aureus* bacteria along with zone of inhibition (mm).

50 µg/ml	100 µg/ml	200 µg/ml	500 µg/ml
14	18	22	25



Symbolic Characteristics of Social Class in Contemporary Architecture of Iran, Case study Tehran.

Mohammad Dana Salem^{1*}, Sohaib Dehghani² and Amir Bahmani Chahestani³

¹Department of Architecture, Islamic Azad University, Marivan Branch, Marivan, Iran.

²Department of Architecture, Tarbiat Modarres University, Tehran, Iran.

³ Faculty of Architecture, Iran Technical and Vocational University Bandar Abbas Branch.

Received: 15 April 2014

Revised: 10 May 2014

Accepted: 29 May 2014

*Address for correspondence

Mohammad Dana Salem,
Department of Architecture,
Islamic Azad University,
Marivan Branch, Marivan, Iran.
E.mail: h.hasani1360@gmail.com.



This is an Open Access Journal / article distributed under the terms of the **Creative Commons Attribution License** (CC BY-NC-ND 3.0) which permits unrestricted use, distribution, and reproduction in any medium, provided the original work is properly cited. All rights reserved.

ABSTRACT

City is living organism and like any other living organism reacts to environmental stimulation. It's life depend on its inhabitants. Inhabitants are scattered around the city based on their social group, their residence and distribution is associated with their social and economical group. The main hypothesis of this study is that different social, economic and cultural groups will influence on the view of cities. In other word, residence with specific social group shapes the neighborhood. The main research questions are: 1-Does the different social groups in cities affect the physical body of city? 2- What is the relation between residential building façade and their inhabitant's social group? In this study, the correlation method is used to determine the relation between two variables, the social status of residents and residential buildings façade. The sample consisted of a random sample of hundreds of residential buildings in district 2 and 12 in Tehran. Residence of both districts is from high and middle class social groups. The results show that different social groups are effective in the shaping of building facades.

Keywords: Community, Social groups, Building facades, Physical body of cities.



Mohammad Dana Salem *et al.*

INTRODUCTION

In this approach the city is described as a social reality. The city is ultimately resultant of relationships between social actors. Therefore, it is believed that the urban space formation follows that too. Sociology is science of recognition and analysis of the "closed society". Based on sociology, society is which people are involved in the formation of culture and social relations (Fakohy, 2010).

Research questions

- Does the different social groups in cities affects the physical body of city?
- What is the relation between residential building façade and their inhabitant's social group?

METHODOLOGY

In this study, the correlation method is used to determine the relation between two variables, the social status of residents and residential buildings façade. Data collection in this study was library method for accessing the theoretical literature on the subject and survey method for physical data collection of neighborhoods (Grout and Wang, 2005).

Society and social groups

Sociology is interested to demonstrate and explain the facts of human acts and practices of a particular group. These interests range from the rise and fall of civilizations throughout the centuries to a riots over several hours (Albrv, 2001). Several factors can be effective in measuring social status, these factors include: race and ancestry, education and career status.

Marxian and Weberian theory of social stratification can be identified in sociology. In Marxian theory, economical factor is the determining factor in social group selection. While the Weberian theory use social status as determining factor. Weber uses the "Status" to distinguish people in society which it contributes to the manifestation of power in society. Status generally refers to the respect and dignity of the individual in society and usually is evaluated in terms of education, employment status, ancestry individuals (Samim and Fatemi, 2007). In other words, social status has a direct link to individuals with respect and dignity in society. In this study, the Weberian theory was used to determine the social status of Tehran residence.

City and social differences

City is dynamic and evolving phenomenon, thus appearance of the city has the same features and will be constantly changing. These environments are dynamic and not static and based on it, this process should be considered in design, build and management process of city (RezaZadeh, 2010). The city is a type of social organization in forming space which produces culture. Also we should consider city as the best context for "culturalization (socilaization)". The city creates subcultures in continuous process from dominant culture of the city by dividing the social labor in specific social groups (RezaZadeh, 2010). In fact, the city is a place where culture is created or modified and also the forces which can change culture born. Subcultures can be adapted to the main zoning of city. Although it's best example can be found in residential zones like neighborhoods. Residential function, the function type of housing can quickly create sub cultural groups. This is known as "neighbor" or "neighborhood" in urban anthropology. Neighbors have continuous desire to cohesion and integration their cultural patterns. This process is consistent with the uptake of aligned and exclusion of non-aligned elements. Therefore sub cultural groups can be found in the upper tissues

**Mohammad Dana Salem et al.**

villa in the city, wealthy elite in residential complexes, middle classes in residential complexes and poor classes in slums. This kind of subculture can also form an element of city like an "alley", a "street", a "neighborhood" or even a "zone" Urban.

Physical characteristics of Tehran

Teheran is the capital of Iran and Tehran Province. With a population of about 8,300,000 and about 14 million metropolitan area, it is Iran's largest city and urban area, and one of the largest cities in Western Asia. In the 20th and 21st centuries, Tehran has been the subject to mass migration of people from all around Iran. The city of Tehran is divided into 22 municipal districts, each with its own administrative centres. The city is home to many historic mosques, churches, synagogues and Zoroastrian fire temples. Contemporary Tehran is a modern city featuring many structures, of which the Azadi (Freedom) Tower and the Milad Tower have come to be symbols of Tehran itself. Tehran is ranked 29th in the world by the population of its metropolitan area.

Analysis of samples

At this stage, both the 2 and 12 district residential building facades were analyzed. Due to the high statistical population, 50 samples from each district were selected as statistical sample and were compared. The study concludes by summarizing the results of the two samples. The façade of buildings in 2 districts were compared in four parts: Entrance and facade form, Elements used in the facade and entrance, Entrance structure, Entrance shape and proportions.

Entrance and facade form

The designs of entrance and facade forms in district 2 are fluid form with the use of curved shapes combined with straight and diagonal shapes. This forms will make entrance pleasant to eye and has inviting effect on people. Fluid forms and curves can represent the variety ambition, greed and the soft mood of the residents. On the other hand, people of lower class area (area 12) are less likely to use rounded corners and curved forms. So that the residents of these areas mostly use other forms like straight and prefer to rectangular forms for their building.

Buildings form in district 2, usually are vertical and high. The reason for this high building are maximum use of land, high price of land and, but it is possible that other factors like showing of the residence and their control over city might be involved. On the other hand most of the buildings in the district 12 are horizontal and low. Low height of the buildings in these areas could be based more on people's economical ability. Entrances in district 2 mostly are above ally's level, thus an upward access element like stairs were used. Although most of entrances in district 12 were under ally's level, thus the accesses were downward. Culture in affluent areas of the city (district 2) is most aristocratic and royal life, So Santouri forms and motifs of ancient Persia have been used in the facade and entrance of the buildings. While the 12 district entrance forms and facades are quite simple and almost devoid of ornamentation.

Elements used in the facade and entrance

In the survey, it had been seen buildings in the district 2 are often decorated with plants. The coating takes place in line with the emphasis on guiding and inviting aspect of the entrance. Most importance of these green spaces is to help with distinguishing between private and public space. Also it will provide a pleasant view for residence while entering or exiting the building. Although in district 12, use of plants were divided in two category, the first which there is no use of plants in entrance and second, plants are inside the building and hidden from public view. The cultural, social and economic differences between district 2 and 12, not only had effected the entrances and facades but also effected the difference in security means, material and quality of construction. The weak economic residence

**Mohammad Dana Salem et al.**

cannot afford to use expensive material and means. In the district 2 fences are located on the entrance door which has an unpleasant view and also show the lack of security in the area. On the other hand in district 12 fences are hidden behind the door.

Entrance structure

In district 2, access to building's interior from entrance can be achieved with two ways. One straight from outside to inside and other one there is courtyard between inside and outside which residence should cross first. In first kind access there is difference elevation between entrance and street which can be achieved by stairs but in the second kind access entrance has the same elevation as street. In district 12, the entrances are mostly solid with no transparency and the elevation mostly is same as street or lower. District 2 entrances mostly have a pre-space before the inside door. This space has a pause and inviting aspect. This space most of the times has ornaments and specific lighting which will increase its inviting aspect. But in district 12, entrances have no pre-space and the door is attached to the street. There is one element which is used in both districts with the same intention but in district 2, this element is more impressive than district 12. Use of columns in entrance increases the visual solidity, strength and also adds to the readability of the entrance.

Almost all the buildings' entrances of district 2 have different access for cars and pedestrians which emphasize the entrance and its user's importance. On the other hand entrance in district 12 has no car parking or car access, at most there is enough space for bikes inside the building. Vertical proportions and the building height help to emphasize the entrance in district 2. In other words all elements and parts in façade try to emphasize the entrance and make it seem more important. While there are much less emphasizing in district 12 which is the residence of low status social groups. Entrances' doors are wide and high in district 2 which has an inviting aspect while the doors in district 12 are small and inferior to district 2 doors. In some cases the measurement of these doors are so small that a common man is barely able to go through it. The apparent differences between the two districts can be seen on the facade as additional elements which are attached to the façade like air conditioning, air conditioner channels and installations, chimneys, gas pipes, labels and signs and advertising, which is not found in district 2 or less found. Appearances of these elements on the façade have an unpleasant view for residents and other people using the street.

Cleanliness of entrance in district 2 was outstanding and was one of the first things understood by the observer. A clean entrance has a very effective influence on the viewer's ability to remember the building and its aspect. While there is much less attention to clean entrance in district 12. High level of economic capacity of residents will improve the quality of façade and entrance. The quality and pleasantness of façade and entrance is high in district 2 whose residents are in a rich economic group. While residents of district 12 are in a low economic group, therefore the quality of façade and entrance is very low and has an unpleasant effect on the neighborhood. Like broken stairs and glasses and damaged elements on the facade. Usage of warm colors on facades, especially in the entrances has an inviting and pleasant effect on people. Usage of warm colors is more in district 2 than in district 12, façade and entrances in district 12 mostly use cold colors.

CONCLUSION

The analysis of the samples and comparison between two districts in Tehran, clearly showed the differences in facades and entrance residential which these differences are influenced by differences in social, cultural, economic, and political status of residents. The differences in urban population have been analyzed by sociologists. As mentioned in the Marxian theory, economic factors should be considered as determinants of the social group of individuals while the Weberian theory of social status should be considered as a social stratification factor. The city's distinct social groups are directly affecting the form and structure of the city. In Tehran, the difference is clearly seen in multiple areas, in this study a comparative table was developed to analyze the difference of two districts. Compared factors were the form of building, dynamic or static forms and well-known forms, colors and materials, plant's use, number of floors, the entrance area, and security means of building. The underlying factors of differences were found



Mohammad Dana Salem et al.

in differences social status of residence. The study confirmed sociologist’s theory on social differences will form the city differently. In other words, the city is a manifestation of social differences and this gap between downtown and suburban areas is quite understandable, especially in Tehran.

REFERENCES

1. Azad Armaki, (2010): "Sociological Theory", Tehran, Sixth Edition, Soroush Publishing Co.
2. Albero Martin, (2001): "Basics of Sociology", translated by M. Saburi, Tehran, First Edition, Nei Publishing Co.
3. Fakohi Naser, (2010): "Urban Anthropology", Tehran, sixth edition, published straw.
4. Grout Linda, Wang David, (2005) "Research Methods in Architecture", translated by Alireza Einifar, Tehran, Tehran University Publishing Co.
5. Reza Zadeh, R. (2010): "Social and cultural factors affecting the quality of urban architecture and landscape", Abadi Quarterly, No. 66, pp. 38-42.
6. Fatemi Sasan, Samim Reza, (2007): "On the sociological study of music among people of different social base", Fine Art Journal, No. 32, pp. 127-135.
7. URL1- (<http://www.tehran.ir/Default.aspx?tabid=117>)(2011-November)

Table 1: Comparison of analytical facade and entrance in District 2 and 12 of Tehran.

Descriptions	District 12	District 2	Analysis element	
curves and fluid form is more interesting this form often reflects the luxurious oriented life Height of the building is a kind class distinction	Static form (flat)	Dynamic Form (fluid)	Movement	Form
	The lack of the known forms	European forms as Santouri	Shape	
	Plain work	Iranian motifs and motifs of ancient aristocratic	Direction	
	Downward motion	Upward motion	Height	
Usually two-storey	More than four storey			
This coverage is also in line with the emphasis on guiding the residents and helps to separate the public and private domains	Empty of plant	Combined with plants	Plant	element
	fenced	Using the security camera	Supervision	
Economic feasibility of using expensive materials not provided for all residents of city entrance above the street guide people and invite people to the building, also give residence an sense of importance Use column in entrance increase the visual solidity, strength and also adds to the readability of the entrance	cheap materials	Expensive materials	Materials	Structure
	Lack of metallic luster	Material with metallic luster	Coating	
	Lack of natural stone	The use of natural stone	Facade	
	downward stair	upward stair	Stair	
no use of column input	Emphasis on the use of the column as entrance	Column		
Transparency of entrance connects the private and public domains	lack of transparency	Promote the visibility and transparency of entrance	Transparency	
Pre-space has an pause and call effect the importance of giving respect to residents by adding pedestrians	Without the pre-space	entrance with pre-space and stairs	Between spaces	Shape
	Bike access	Car access	Access	
	No separation of car and walk access	Separation of car and walk access		
vertical proportions helps to emphasizes the entrance	Horizontal proportion	Vertical proportion	Proportions	
Spacious entrances emphasizes the inviting effect of building	The separation of facade and entrance	Emphasis on the entrance	Facade	Shape
	Short and narrow doors	Large and drawn doors	Doors	
Ugly and unpleasant aesthetic point of view and for residences	additional elements on the facade	No additional elements on the facade	Additional element	
The importance of entrance as first encountering element of building	Lack of acceptable deans	Sanitation and clean entrance and facade	Cleanses	Shape
	Home and entrance without privacy elements	privacy of the home and entrance	Privacy	
Rich economy will improve the quality of facade and entrance	poor build quality	high build quality	Quality	



Figure 1 - Curved forms in a district 2, entrance House entrance



Figure 2 - Straight forms in a district 12 House,

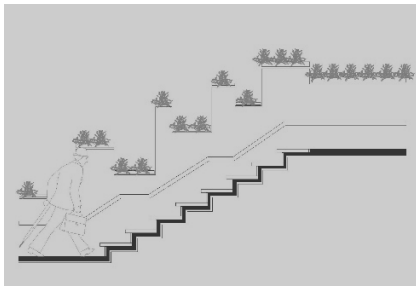


Figure 3 - entrance higher than street level.



Figure 4 - entrance lower than street level .



Figure 5 - Entrance buildings often with plants, District 2.



Figure 6 - Entrance vacant from ecological qualities, District 12.



Mohammad Dana Salem *et al.*



Figure 7 - Lack of plants in front of the entrance but behind the door,

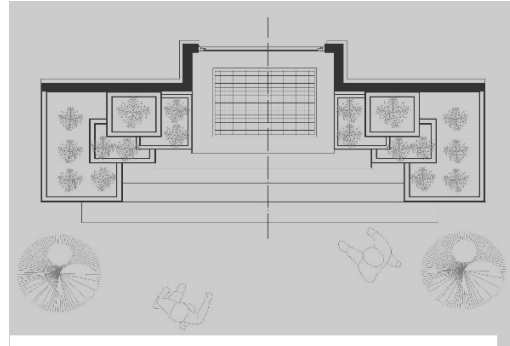


Figure 8 - plants in front of the entrance which has inviting and guiding effect.



Figure 9 - Access from the bottom to up, it shows the importance of residents (upward).

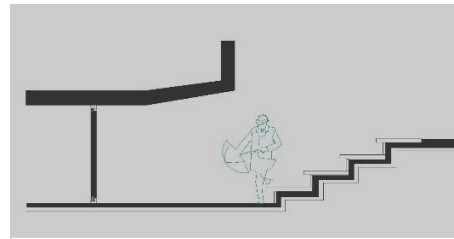


Figure 10 - Access from the up to bottom (downtrend).

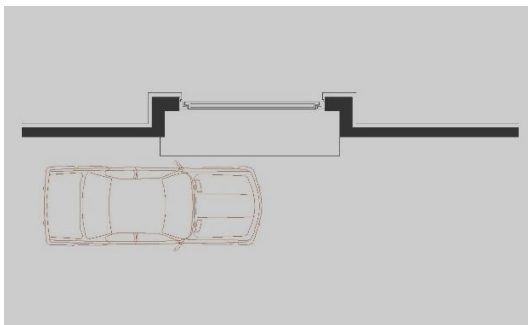


Figure 11 - entrance as being on a par with the building and the lack of emphasis on it.

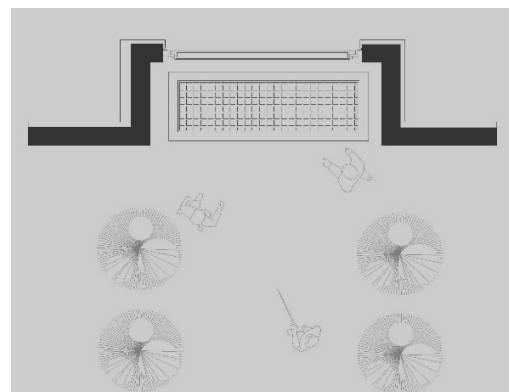


Figure 12 - the entrance sit back in to the building (emphasizing the entrance and make it inviting).



Mohammad Dana Salem *et al.*



Figure 13 – Emphasizing on entrance by column and pre-space, District 2.



Figure 14 - Entrance par with street and without column, District 12.

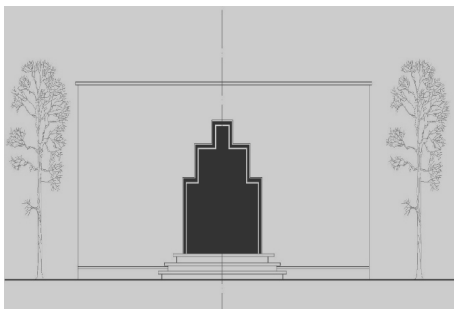


Figure 15 - The different materials of entrance with inviting sense.

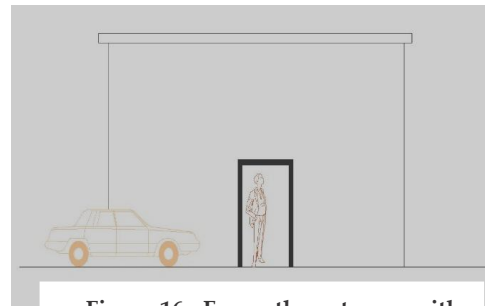


Figure 16 - Frame the entrance with different materials and the lack of emphasis on it.



Figure 17 - Vertical proportions and height of the door emphasis the entrance, District 2.



Figure 18 – less emphasizing on the entrance, District 12.



Mohammad Dana Salem et al.



Figure 19 - Using a large entrance doors.

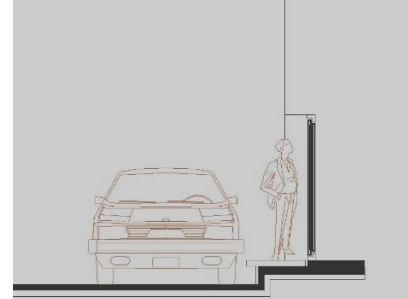


Figure 20 - Short, narrow entrance doors.



Effect of Transportation on the Behaviour, Body weight and Carcass Traits of Halothane Sensitive Pigs.

Manju Sasidharan^{1*} and P.C.Saseendran²

¹Department of Livestock Production Management, College of Veterinary and Animal Sciences, Pookode, Wayanad -673576, Kerala,India.

²Department of Livestock Production Management, College of Veterinary and Animal Sciences, Mannuthy, Trichur -680651,Kerala,India.

Received: 21 April 2014

Revised: 18 May 2014

Accepted: 30 May 2014

*Address for correspondence

Manju Sasidharan
Department of Livestock Production Management,
College of Veterinary and Animal Sciences,
Pookode,Wayanad -673576,
Kerala,India.
E.mail: manju@kvasu.ac.in



This is an Open Access Journal / article distributed under the terms of the **Creative Commons Attribution License (CC BY-NC-ND 3.0)** which permits unrestricted use, distribution, and reproduction in any medium, provided the original work is properly cited. All rights reserved.

ABSTRACT

A study to assess the effect of transportation on the behavior, body weight and carcass traits of halothane sensitive pigs was carried out. Twenty four weaner piglets were selected after screening for halothane sensitivity. Twelve piglets, six from halothane positive and six from halothane negative were transported. Mixing of different treatment groups during transportation resulted in fights between the genotypes, the halothane negative being more aggressive. Shrinkage due to transport at 90days of age showed significant difference ($P<0.01$) between the halothane genotypes. The halothane resistant pigs had higher loss in body weight than sensitive pigs. At 210 days of age, the difference in loss in body weight between halothane genotypes were not significant ($P<0.05$). The carcass traits like carcass weight after beheading, dressing percentage, carcass length, loin eye area and back fat thickness did not differ between the genotypes or between the transported and non-transported group. There was significant difference ($P<0.01$) in meat pH between the halothane genotypes and between transported and non-transported groups. The higher meat pH values observed in non-transported groups were indicative of better meat quality.

Key words: Halothane sensitivity, Transportation, Behaviour, Shrinkage, Carcass traits, Meat pH

**Manju and Saseendran****INTRODUCTION**

Welfare problems arise for pigs if they are unable to control events in their environment. Such events include physical abuse, neglect, handling, transport and diseases. Some pigs suffer from extreme susceptibility to stress, controlled by a single recessive gene the halothane gene. Ever since the halothane gene was first identified, numerous studies have been conducted to compare carcass and meat quality characteristics of halothane genotypes. Commercially the halothane gene is of interest because it results in increased carcass lean contents (Aalhus *et al.*, 1991; Pommier *et al.* 1992) [1,2]. However halothane reactors (nn) in comparison with negative animals (NN), are more stress susceptible and produce poor meat quality, particularly in terms of higher incidence of pale soft exudative meat. In pig farms, transportation is mainly at two stages, viz., at weaning stage and marketing stage of fattening pigs. During transport or mixing of weaners, vigorous fighting resulted in weight loss. Reports on the transportation loss of pigs reared by farmers seem to be limited. Since a large number of pigs are transported from farms to abattoirs, there is a need to study the effect of transportation on the carcass traits of pigs. Pre-slaughter stress such as fighting, cold weather, fasting and transportation depletes muscle glycogen of finishing pigs resulting in meat which has higher p^H due to lack of lactic acid production (Grandin, 1980) [3]. The present study was conducted to find the changes in behaviour, body weight and carcass traits of halothane sensitive pigs.

MATERIALS AND METHODS

Twelve halothane positive and twelve halothane negative pigs were selected at random after halothane test. The pigs aged three to eleven weeks and weighing upto 26kg were gently restrained and allowed to breathe halothane in oxygen via a face mask for up to three minutes. Reactions were assessed visually as the degree of rigidity of hindlegs and were scored as positive (nn), doubtful (Nn) or negative (NN) where a positive reaction was defined as extreme rigidity. Pigs reacting positively to halothane anesthesia had considerably elevated body temperature, increased frequency of respiration and pulse and tonic muscular contraction of limb extensors within three minutes of halothane administration. Pigs not reacting to halothane did not show these symptoms throughout the four minutes of halothane administration (Bulla *et al.* 1991) [4]. The pigs were assigned to four treatment groups as given below.

Group I-Six halothane negative pigs subjected to transportation.

Group II- Six halothane positive pigs subjected to transportation.

Group III-Six halothane negative pigs not subjected to transportation.

Group IV-Six halothane positive pigs not subjected to transportation.

The pigs were housed in identical sties with concrete flooring and each having a covered area of 6.1m². All the sties had access to exercise yards with wallowing tank and were cleaned daily.

The body weight of each group was observed before and after transportation. Transportation was done in an open truck at 90 days and 210 days of age. A floor space of 0.5 m² was provided per animal. The vehicle halted twice during transport, after two hours and four hours. The behavioural changes of the animals were observed during transport. The animals were slaughtered after transport. Live body weight at slaughter, carcass weight after beheading, dressing percentage, carcass length, loin eye area and back fat thickness were measured. Carcass length was measured as the straight line distance from the pubic symphysis to the anterior edge of the first rib taken on a suspended carcass (Kridler and Carroll, 1971) [5]. The loin eye area was calculated by making the outline of longissimus dorsi muscle between the tenth and eleventh rib (Kridal and Carroll, 1971) [5]. The backfat thickness was measured at several points at the first rib, last rib and last lumbar vertebra and the average is taken. The pH of meat from Rectus femoris muscle was estimated using the pH meter 45 minutes after slaughter. The data was analysed by Snedecor and Cochran (1967) [6].

**Manju and Saseendran****RESULTS AND DISCUSSION**

At the time of transportation at 90 days of age both the halothane positive and negative animals were in standing posture. The animals stood parallel to the direction of transit or perpendicularly, with their sides touching each other. When the vehicle stopped after two hours, the halothane negative animals attacked more frequently and within few minutes after the halt vigorous fighting were seen among the pigs. Fighting stopped when the vehicle started running and all the animals were in standing posture. When the vehicle halted again after three hours all pigs except one negative pig lied down. The animals stood up again when the vehicle started .After four hours, most of the positive pigs had drooling of saliva and increased respiration rate.

During transportation at 210 days of age, fighting was observed as soon as halothane positive and negative pigs were mixed before loading. Both the genotypes exhibited increased respiratory rate after loading .Panting and drooling of saliva were observed for all animals within half an hour of transport. After one hour journey the animals started lying down. Even when the vehicle stopped, there was no change in the behaviour .All seemed to be under stress and had frothy drooling of saliva. This continued till the animals were unloaded at the slaughter house. In the lairage, the animals preferred to be in the wallowing tank even after one hour. Though the place was a novel environment the pigs didn't show any investigatory behaviour and was resting.

Live weight of pigs before and after transportation showing the weight loss caused by transportation stress is shown in table 1. Though the body weights before and after transportation at 90 days of age and 210 days of age did not differ significantly between the halothane genotypes, the loss of weight due to transport showed significant difference between the two groups at 90 days of age. The halothane resistant pigs had a higher loss in body weight than sensitive pigs (Table 1). The mean losses in body weight for halothane resistant pigs were 2.00 ± 0.22 kg and for sensitive pigs were 1.083 ± 0.24 kg. The percentage weight losses were 11 ± 0.503 and 6.847 ± 1.32 respectively.

At 210 days of age , the loss in body weight was insignificant. The halothane negative animals lost 5.1 ± 0.4 kg and halothane positive animals lost 3.417 ± 0.61 kg. bodyweight respectively. The percentage loss in body weight were 7.206 ± 0.813 for halothane resistant and 5.328 ± 0.82 for halothane sensitive animals .In the case of non-transported halothane negative and positive pigs the average dressed weight after beheading were 47.75 ± 4.72 and 46.83 ± 4.26 kg respectively. For transported pigs the halothane negative and positive pigs had a mean weight of 48.8 ± 3.84 kg and 44.83 ± 2.54 kg. The difference between the treatment groups was insignificant.

The carcass length, dressing percentage, loin eye area and back fat thickness of the treatment groups were given in table 2 .There was no significant difference between the transported and non –transported groups and between the genotypes. Halothane positive pigs and the transported pigs had shorter carcasses than the halothane negative and non-transported pigs. The shorter carcasses due to halothane genotype were observed by Wittman *et.al.* (1993)[7]. In both transported and non-transported pigs, halothane negative pigs had higher dressed weight than halothane positive pigs. In dressing percentage no trend towards any group could be observed .The result of the study was in confirmation with reports of Sather *et.al.* (1991)[8]. Contradicting results were obtained by Rundgren *et.al.* (1990)[9] with higher dressing percentage for reactors. The dressing percentage of 77.44 obtained for transported pigs were similar to that obtained by Kortz *et.al.* (1995)[10] when pigs were transported for more than 50 km.

Loin eye area was higher in halothane positive pigs among non-transported group and lower in transported but the difference was non-significant. The non-significant differences of loin eye area between genotypes were observed by Leach *et.al.* (1996)[11]. The lowest backfat thickness of 23.5 ± 0.18 mm was observed in non-transported halothane positive pigs and the highest of 29.1 ± 0.3 mm backfat thickness for transported halothane positive pigs. But no trend due to genotype and transport on backfat thickness could be observed. This was supported by the findings of Leach *et.al.* (1996), Franco *et.al.* (2008), Yang *et.al.* (2012)[11-13].



Manju and Saseendran

The average meat p^H of non-transported halothane negative and positive animals was 6.52 ± 0.074 and 5.81 ± 0.06 and that of transported pigs were 5.72 ± 0.08 and 5.56 ± 0.21 respectively. The mean of halothane negative group was 6.07 ± 0.15 and for halothane positive genotype was 5.69 ± 0.11 . The meat pH of non-transported halothane negative pigs varied significantly from the meat pH of transported halothane negative and positive pigs. There was significant difference in meat pH between the two halothane genotypes and between the transported and non-transported groups. The lower pH observed for the halothane positive pig in the present study was in agreement with the result obtained by Sencic *et.al.* (1989), Fewson *et.al.* (1993) [14,15]. Even though there was no appreciable visual changes to the carcass indicating pale soft exudative (PSE) meat in any of the groups studied the lowered pH may be indicative of the reactors susceptibility for developing PSE meat. The reactors appear vulnerable to stress as significantly lower pH ($P < 0.01$) has been observed among pigs subjected to transport before slaughter. Poor meat quality in halothane reactors had been observed by Leach *et.al.* (1996). Kortz *et.al.* (1995) [11,10] observed a superior meat quality among pigs transported for shorter distances than the pigs transported for longer distances. The study showed that transportation immediately before slaughter resulted in lowered meat pH which had an adverse effect on meat quality.

REFERENCES

1. Aalhus, J.L., Jones, S.D.M., Robertson, W.M., Tong, A.K.W. and Sather, A.P. 1991. Growth characteristics and carcass composition of pigs with known genotypes for stress susceptibility over a weight range of 70 to 120 kg. *Anim. Prod.*, 52:347.
2. Pommier, S.A., Houde, A., Rousseau, F. and Savoie, Y. 1992. The effect of malignant hyperthermia genotype as determined by a restriction endonuclease assay on carcass characteristic of commercial crossbred pigs. *Can. J. Anim. Sci.* 72:973-976.
3. Grandin, T. 1980. The effect of stress on livestock and meat quality prior to and during slaughter. *International Journal for the study of Animal problems*. 1:313-337.
4. Bulla, J., Bullova, M., Kolataj, A. 1991. Some etiological and physiological indicators of MHS in pigs. *J. Anim. Breed. Genet.* 108:315-318.
5. Krider, J.I. and Carroll, W.E. 1971. Swine Production, 4th Edition Tata Mcgraw-Hill Publishing Company Ltd. pp: 63-70.
6. Snedecor, G.W. and Cochran, W.G. 1967. Statistical Methods, 6th Edition. The IOWA State University Press, Amer, USA.
7. Wittmann, W., Peschke, W., Littmann, E., Behringer, J., Birkenmaier, S., Dove, P., Forster, M. 1993. Finishing and Carcass traits of German Landrace Barrows in relation to MHS genotype *zuchtungskunde* 65:197-205.
8. Sather, A.P., Murray, A.C., Zawadski, S.M., Johnson, P. 1991. The effect of Halothane gene on pork production and meat quality of pigs reared under commercial conditions. *Can. J. Anim. Sci.* 71:959-967.
9. Rundgren, M., Lundstrom, K., Elfors-Lilja, 1990. A within litter comparison of the three halothane genotypes Performance, carcass quality, Organ development and long term effects of transportation and amperozide treatment. *Livest. Prod. Sci.* 26:231-243.
10. Kortz, J., Karamucki, T., Gardzielewska, J., Szafran, E. 1995. Characteristics of porkers bred on private farms and on meat industry-owned farms in relation to different distances of transportation to the slaughter house. *Adv. Agric. Sciences.* 4:55-61.
11. Leach, L.M., Ellis, M., Sutton, D.S., Mckieth, F.K., Wilson, E.R., 1996. The growth performance, carcass characteristics and meat quality of halothane carrier and negative pigs. *J. Anim. Sci.* 74:934-943.
12. Franco, M.M., Antunes, R.C., Borges, M., Melo, E.O., Goulart, L.R. 2008. Influence of Breed, Sex and Growth hormone and halothane genotypes on carcass composition and meat quality traits in pigs. *Journal of Muscle Foods.* 19(1):34-49.
13. Yang, Y., Guo, J., Kim, J.S., Wang, M.H., Chae, B.J. 2012. Effect of growth rate on carcass and meat quality traits and their association with metabolism-related expression in finishing pigs. *J. Anim. Sci.* 83(2):169-177.



Manju and Saseendran

14. Sencic, D., Petricevic, A., Kralic, G. 1989. Stress in pigs and Meat quality, *Stocarstvo* 43:259-268.
15. Fewson, D., Rathfeldor, A., Muller, E. 1993. Investigations on the correlations between the percentage of carcass lean, meat quality and stress resistance in pigs of different genetic origin. 1. Importance of the morphology of the eye muscle. *Anim. Breed. Abstr.* 62(4):2038.

Table1. Mean shrinkage during transportation of pigs.

Parameters	Age			
	90 days		210 days	
Genotype	Halothane (-ve)	Halothane (+ve)	Halothane(-ve)	Halothane(+ve)
Bodyweight before transportation(kg)	18.00±1.41	15.42±0.76	72.30±4.70	63.92±3.69
Body weight after transportation(kg)	16.00±1.20	14.33±0.63	67.20±4.85	60.50±3.47
Weight loss (kg)	2.00±0.22*	1.08±0.24*	5.10±0.40	3.41±0.61
Body weight lost (%)	11.00±0.50*	6.84±1.32*	7.20±0.81	5.32±0.82

*Significantly different at 1% level.

Table 2. Carcass traits of non-transported and transported halothane resistant and sensitive pigs.

Carcass traits	Non-transported		Transported	
	Halothane (-ve)	Halothane (+ve)	Halothane(-ve)	Halothane(+ve)
Carcass length(cm)	76.00±2.10	75.50±1.84	74.70±1.52	71.17±1.03
Dressed weight(kg)	47.75±4.72	46.83±4.26	48.8±3.84	44.83±2.54
Dressing percentage	71.73±1.52	74.18±1.26	76.18±0.78	78.48±2.57
Meat p ^H	6.52±0.079 **	5.81±0.06	5.72±0.08**	5.56±0.21**
Loin eye area(cm ²)	25.94±2.87	27.82±1.52	23.80±1.12	20.46±0.57
Backfat thickness(mm)	26.48±0.23	23.50±0.18	25.50±0.27	29.10±0.30

** Highly significant P < 0.01

**INSTRUCTION TO AUTHOR (S)**

Manuscripts should be concisely written and conform to the following general requirements: Manuscripts should be type written in double-space in A4 sized sheets, only on one side, with a 2 cm margin on both sides. Research Papers should have more than 15 pages, Review Articles in the range of 15-30 pages and Short Communications up to 15 pages, inclusive of illustrations. Pages should be numbered consecutively, starting with the title page and the matter arranged in the following order: Title page, Abstract, Introduction, Materials and Methods, Results, Discussion or Results and Discussion, Acknowledgements, References, Illustrations (Tables and figures including chemistry schemes along with titles and legends) and figure and Table titles and legends. Abstract should start on a separate page and each table or figure should be on separate sheets. The titles "Abstract" and "Introduction" need not be mentioned. All other section titles should be in capital letters while subtitles in each section shall be in bold face lower case followed by a colon.

Title Page - Title page should contain title of the paper in bold face, title case (font size 14), names of the authors in normal face, upper case (font size 12) followed by the address(es) in normal face lower case. The author to whom all correspondence be addressed should be denoted by an asterisk mark. The title should be as short as possible and precisely indicate the nature of the work in the communication. Names of the authors should appear as initials followed by surnames for men and one given-name followed by surname for women. Full names may be given in some instances to avoid confusion. Names should not be prefixed or suffixed by titles or degrees. Names should be followed by the complete postal address or addresses with pin code numbers of the place(s), where the research work has been carried out. At the bottom left corner of the title page, please mention "*Address For correspondence" and provide a functional e-mail address. Address of the corresponding author to whom all correspondence may be sent should be given only if it is different from the address already given under authors' names. Trivial sub-titles such as 'Title', 'Author', 'Address' or 'Place of Investigation' shall not be included in the title page. Title page should be aligned centre except for "* Address For correspondence". Provide a running title or short title of not more than 50 characters.

Abstract - Should start on a new page after the title page and should be typed in single-space to distinguish it from the Introduction. Abstracts should briefly reflect all aspects of the study, as most databases list mainly abstracts. Short Communications as well as Review Articles should have an Abstract.

Key-words - Provide four to ten appropriate key words after abstract.

Introduction - Shall start immediately after the Abstract, as the next paragraph, but should be typed in double-space. The Introduction should lead the reader to the importance of the study; tie-up published literature with the aims of the study and clearly states the rationale behind the investigation.

Materials and Methods - Shall start as a continuation to introduction on the same page. All important materials used along with their source shall be mentioned. The main methods used shall be briefly described, citing references. Trivial details may be avoided. New methods or substantially modified methods may be described in sufficient detail. The statistical method and the level of significance chosen shall be clearly stated.

Results - All findings presented in tabular or graphical form shall be described in this section. The data should be statistically analyzed and the level of significance stated. Data that is not statistically significant need only to be mentioned in the text - no illustration is necessary. All Tables and figures must have a title or caption and a legend to make them self-explanatory. Results section shall start after materials and methods section on the same page.



INSTRUCTION TO AUTHOR(S)

Discussion - This section should follow results, deal with the interpretation of results, convey how they help increase current understanding of the problem and should be logical. Unsupported hypothesis should be avoided. The Discussion should state the possibilities the results uncover, that need to be further explored. There is no need to include another title such as "Conclusions" at the end of Discussion. Results and discussion of results can also be combined under one section, Results and Discussion.

Acknowledgements - Should be given after the text and not in the form of foot-notes.

References - Should be numbered consecutively in the order in which they are first mentioned in the text (not in alphabetic order). Identify references in text, tables, and legends by Arabic numerals in superscript in square brackets. References cited only in tables or figure legends should be numbered in accordance with the sequence established by the first identification in the text of the particular table or figure. Use the style of the examples below, which are based on the formats used by the international journals. The titles of journals should be abbreviated according to the style used in international journals. Use complete name of the journal for non-indexed journals. Avoid using abstracts as references. Information from manuscripts submitted but not accepted should be cited in the text as "unpublished observations" with written permission from the source. Avoid citing a "personal communication" unless it provides essential information not available from a public source, in which case the name of the person and date of communication should be cited in parentheses in the text. For scientific articles, contributors should obtain written permission and confirmation of accuracy from the source of a personal communication. The commonly cited types of references are shown here, for other types of references such as electronic media; newspaper items, etc. please refer to ICMJE Guidelines (<http://www.icmje.org>).

Articles in Journals

1. Devi KV, Pai RS. Antiretrovirals: Need for an Effective Drug Delivery. Indian J Pharm Sci 2006;68:1-6.
List the first six contributors followed by *et al*.
2. Volume with supplement: Shen HM, Zhang QF. Risk assessment of nickel carcinogenicity and occupational lung cancer. Environ Health Perspect 1994; 102 Suppl 1:275-82.
3. Issue with supplement: Payne DK, Sullivan MD, Massie MJ. Women's psychological reactions to breast cancer. Semin Oncol 1996;23(1, Suppl 2):89-97.

Books and other Monographs

4. Personal author(s): Ringsven MK, Bond D. Gerontology and leadership skills for nurses. 2nd ed. Albany (NY): Delmar Publishers; 1996.
5. Editor(s), compiler(s) as author: Norman IJ, Redfern SJ, editors. Mental health care for elderly people. New York: Churchill Livingstone; 1996.
6. Chapter in a book: Phillips SJ, Whisnant JP. Hypertension and stroke. In: Laragh JH, Brenner BM, editors. Hypertension: pathophysiology, diagnosis, and management. 2nd ed. New York: Raven Press; 1995. p. 465-78.

Illustrations: Tables - Should be typed on separate sheets of paper and should not preferably contain any molecular structures. Only MS word table format should be used for preparing tables. Tables should show lines separating columns but not those separating rows except for the top row that shows column captions. Tables should be numbered consecutively in Arabic numerals and bear a brief title in capital letters normal face. Units of

**INSTRUCTION TO AUTHOR(S)**

measurement should be abbreviated and placed below the column headings. Column headings or captions shall be in bold face. It is essential that all tables have legends, which explain the contents of the table. Tables should not be very large that they run more than one A4 sized page. Tables should not be prepared in the landscape format, i. e. tables that are prepared width wise on the paper.

Figures - Should be on separate pages but not inserted with in the text. Figures should be numbered consecutively in Arabic numerals and bear a brief title in lower case bold face letters below the figure. Graphs and bar graphs should preferably be prepared using Microsoft Excel and submitted as Excel graph pasted in Word. These graphs and illustrations should be drawn to approximately twice the printed size to obtain satisfactory reproduction. As far as possible, please avoid diagrams made with India ink on white drawing paper, cellophane sheet or tracing paper with hand written captions or titles. Photographs should be on glossy paper. Photographs should bear the names of the authors and the title of the paper on the back, lightly in pencil. Alternatively photographs and photomicrographs can be submitted as jpeg images. Figure and Table titles and legends should be typed on a separate page with numerals corresponding to the illustrations. Keys to symbols, abbreviations, arrows, numbers or letters used in the illustrations should not be written on the illustration itself but should be clearly explained in the legend. Avoid inserting a box with key to symbols, in the figure or below the figure. In case of photomicrographs, magnification should be mentioned either directly on them or in the legend. Symbols, arrows or letters used in photomicrographs should contrast with the background. Method of staining should also be mentioned in the legend.

Chemical terminology - The chemical nomenclature used must be in accordance with that used in the Chemical Abstracts.

Symbols and abbreviations - Unless specified otherwise, all temperatures are understood to be in degrees centigrade and need not be followed by the letter 'C'. Abbreviations should be those well known in scientific literature. *In vitro*, *in vivo*, *in situ*, *ex vivo*, *ad libitum*, *et al.* and so on are two words each and should be written in italics. None of the above is a hyphenated word. All foreign language (other than English) names and words shall be in italics as a general rule. Words such as carrageenan-induced inflammation, paracetamol-induced hepatotoxicity, isoproterenol-induced myocardial necrosis, dose-dependent manner are all hyphenated.

Biological nomenclature - Names of plants, animals and bacteria should be in italics.

Enzyme nomenclature - The trivial names recommended by the IUPAC-IUB Commission should be used. When the enzyme is the main subject of a paper, its code number and systematic name should be stated at its first citation in the paper.

Spelling - These should be as in the Concise Oxford Dictionary of Current English.

SHORT COMMUNICATIONS

The journal publishes exciting findings, preliminary data or studies that did not yield enough information to make a full paper as short communications. These have the same format requirements as full papers but are only up to 15 pages in length in total. Short Communications should not have subtitles such as Introduction, Materials and Methods, Results and Discussion - all these have to be merged into the running text. Short Communications preferably should have only 3-4 illustrations.

REVIEW ARTICLES

Should be about 15-30 pages long, contain up-to-date information, comprehensively cover relevant literature and preferably be written by scientists who have in-depth knowledge on the topic. All format requirements are same as



INSTRUCTION TO AUTHOR(S)

those applicable to full papers. Review articles need not be divided into sections such as materials and Methods and Results and Discussion, but should definitely have an Abstract and Introduction, if necessary.

PUBLICATION FEE

To publish the paper in our journal author should be paid **Rs. 2500 (INDIA)** in advance by money transfer or DD drawn in favour of Indian Journal Of Natural Sciences, payable at Indian Bank, Arimalam.*All correspondence relating to subscription and manuscript submission may be address to

Editor in Chief, Indian Journal of Natural Sciences

C/o Tamil Nadu Scientific Research Organization (TNSRO)

39, Mura Bhavan, Koodal Nagar, Rajgopalapuram Post

Pudukkottai -622003, TamilNadu, India Contact Nos: 04322-261088, 9952886637, 9894217573

E.mail: ijonstnsro@gmail.com, editorijons@gmail.com

For open access please visit our official website : www.tnsroindia.org.in



This is an Open Access Journal / article distributed under the terms of the **Creative Commons Attribution License** (CC BY-NC-ND 3.0) which permits unrestricted use, distribution, and reproduction in any medium, provided the original work is properly cited. All rights reserved.